

Quantum Invariants of Links and 3-Manifolds with Boundary defined via Virtual Links: Calculation of some examples

Heather A. Dye, Louis H. Kauffman and Eiji Ogasa

Abstract. In the prequel of this paper, Kauffman and Ogasa introduced new topological quantum invariants of compact oriented 3-manifolds with boundary where the boundary is a disjoint union of two identical surfaces. The invariants are constructed via surgery on manifolds of the form $F \times I$ where I denotes the unit interval. Since virtual knots and links are represented as links in such thickened surfaces, we are able also to construct invariants in terms of virtual link diagrams (planar diagrams with virtual crossings).

These invariants are new, nontrivial, and calculable examples of quantum invariants of 3-manifolds with non-vacuous boundary.

Since virtual knots and links are represented by embeddings of circles in thickened surfaces, we refer to embeddings of circles in the 3-sphere as *classical links*. Classical links are the same as virtual links that can be represented in a thickened 2-sphere and it is a fact that classical links, up to isotopy, embed in the collection of virtual links taken up to isotopy. We give a new invariant of classical links in the 3-sphere in the following sense: Consider a link L in S^3 of two components. The complement of a tubular neighborhood of L is a manifold whose boundary consists in two copies of a torus. Our invariants apply to this case of bounded manifold and give new invariants of the given link of two components. Invariants of knots are also obtained.

In this paper we calculate the topological quantum invariants of some examples explicitly. We conclude from our examples that our invariant is new and strong enough to distinguish some classical knots from one another.

We examine links that are embedded in thickened surfaces and obtain invariants of three manifolds obtained by surgery on these thickened surfaces. One could take the viewpoint that the thickened surfaces are embedded in the three sphere and so also consider the three manifolds obtained by surgery on the links in the three sphere. These two points of view are distinct and give distinct invariants. This point of view for links in thickened surfaces is distinct from the usual point of view for the Reshetikhin-Turaev invariants, and our invariants give distinct results from these invariants. (See the body what kind of viewpoint).

CONTENTS

1. Introduction	2
Part 1. The new quantum invariants v_r: Review of the definition	6
2. Quantum invariants v_r of 3-manifolds with boundary	6
3. Framed links in thickened surfaces	7
4. Framed link representations of 3-manifolds with non-vacuous boundary	11
5. Framed links in thickened surfaces and simply connected 4-manifolds	11
6. Quantum invariants ς_r of framed virtual links: Outline	14
7. Virtual knots and virtual links	15
8. Quantum invariants ς_r of framed virtual links: Review of Definition	19
9. Our topological quantum invariants v_r of 3-manifolds with boundary	25
10. Our topological quantum invariants v_r of classical knots in the 3-sphere	26
Part 2. Calculation	27
11. The simple connectivity condition is necessary to define our quantum invariants v_r	27
12. Framed links in complements of knots	30
13. Framed links in complements of 2-component links	30
14. Our topological quantum invariants v_r is different from the Reshetikhin-Turaev topological quantum invariants τ_r	38
15. Calculation result	42
Appendix	50
References	51

1. Introduction

In the prequel [14] of this paper, Kauffman and Ogasa introduced new topological quantum invariants of compact oriented 3-manifolds with boundary where the boundary is a disjoint union of two identical surfaces, by using *virtual links*. Let v_r denote this topological invariant. Using the topological quantum invariants v_r , they defined invariants of classical knots and links in the 3-sphere. We review the invariant v_r in Part 1.

The set of virtual links is a quotient set of links in thickened surfaces ([8, 10, 11]). We review it in §7. In this paper, a thickened surface means (an oriented closed surface) \times (the oriented interval).

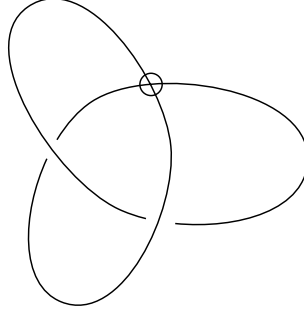


FIGURE 1.1. **The Jones polynomial of this virtual knot is not that of any classical knot.**

Links in the 3-sphere are called *classical links*. There is a natural bijection between the set of links in the 3-spheres and that in the thickened 2-sphere. Therefore the set of classical links is a subset of that of virtual links (In fact, it is a proper subset.). If we apply the definition of the Jones polynomial of virtual links to a classical links, it is the original Jones polynomial of the given classical link. The Jones polynomial of links in thickened surfaces and that of links in the 3-sphere have different properties ([8, 10, 11]): There is a virtual 1-knot whose Jones polynomial is not that of any classical knot. An example is shown in Figure 1.1. A small circle placed around the crossing point as shown in Figure 1.1 is called a virtual crossing. We will review it in §7.

A reason why virtual knot theory is important is as follows. It is an outstanding open question whether we can define the Jones polynomial in any 3-manifolds, although many other invariants are extended to the case of links in other 3-manifolds than the 3-sphere easily. Only one explicit partial answer is given the Jones polynomial for links in thickened surfaces for now. It is given by Kauffman by using virtual links. The Jones polynomial of links in thickened surfaces and that of links in the 3-sphere have different properties as written above ([8, 10, 11]). Note that neither Reshetikhin and Turaev [33, Theorem 3.3.3, page 560] nor Witten[40] answers the above question. See Appendix.

By using virtual links, we constructed a partial answer to the above question. Furthermore, Kauffman and Ogasa [14] used virtual links, and introduced a new topological invariant v_r of classical links as stated in the first paragraph. It is a main theme of this paper to discuss this invariant v_r .

In Part 2 of this paper we calculate the topological quantum invariants v_r of some examples explicitly. We conclude from our examples of explicit calculations that our invariant v_r is new and strong enough to distinguish some classical knots from one another.

Our main theorems are the following two claims.

Theorem 13.2. *Our topological quantum knot invariants v_r are strong enough to distinguish some classical knots from one another.*

Corollary 13.3. *Our topological quantum invariants v_r are strong enough to distinguish some 3-manifolds with boundary where the boundary is a disjoint union of two identical surfaces, from one another.*

We review the new topological quantum invariants v_r below.

When Jones [7] introduced the Jones polynomial, he [7, page 360, §10] tried to define a 3-manifold invariant associated with the Jones polynomial, and succeeded in some cases. After that, Witten [40] wrote a path integral for a 3-manifold invariant. Reshetikhin and Turaev [33] defined a 3-manifold invariant via surgery and quantum groups that one can view as a mathematically rigorous definition of the path integral. Kirby and Melvin, and Lickorish and Kauffman and Lins [20, 23, 24, 12] continued this work. Such 3-manifold invariants are called *quantum invariants* τ_r . These quantum invariants τ_r were defined for closed oriented 3-manifolds. In order to avoid confusion, we let v_r denote our new topological quantum invariant and τ_r the Reshetikhin-Turaev quantum invariant.

In [14] Kauffman and Ogasa introduced topological quantum invariants v_r of compact oriented 3-manifolds with boundary where the boundary is a disjoint union of two identical surfaces. We review it in §9. We explain how to use Kirby calculus for such manifolds, and we use the diagrammatics of virtual knots and links to define these invariants.

Our invariants v_r give new invariants of classical links in the 3-sphere in the following sense: Consider a link L in S^3 of two components.

In this paper, the *complement* of a link means as follows: Take a tubular neighborhood $N(L)$ of L . $N(L)$ is the total space of the open D^2 -bundle over L . The complement is $S^3 - N(L)$.

The complement of a tubular neighborhood of L is a manifold whose boundary consists in two copies of a torus. Our invariants apply to this case of bounded manifold and give new invariants of the given link of two components. We apply the same method and also obtain an invariant of 1-component links. See §13. In this way, the theory of virtual links is used to construct new invariants of classical links in the 3-sphere.

It should be mentioned that the application of virtual knots to the calculation of these invariants is non-trivial and necessary. In [4], Dye and Kauffman defined a quantum invariant for framed virtual links. In order to avoid confusion, we let ς_r denote the Dye-Kauffman quantum invariant. The Dye-Kauffman handling for Kirby calculus and Temperley-Lieb Recoupling Theory for virtual link diagrams allows us to give specific

formulas for our invariants for manifolds obtained by surgery on framed links embedded in a thickened surface. Just as the Jones polynomial can be calculated for links in thickened surfaces via virtual knot combinatorics, so can these surgery invariants be so calculated. Note that in order to apply the virtual diagrammatic Kirby calculus, we need to set our diagrams so that the Roberts circumcission move \mathcal{O}_3 (Figure 4.3) is not needed. This we do by choosing a special surgical normalization as described below. One result of the normalization is that one cannot take any framed virtual diagram for our purposes, but any diagram can be modified so that the normalization is in effect. In this paper we review the definitions and frameworks of [14], and provide specific calculations and applications.

In the sections to follow we address a number of issues. We show how to specify framings for the links in a thickened surface so that one can apply surgery. We explain the results of Justin Roberts [35] for surgery on three manifolds that are relevant and that apply for our use of Kirby Calculus. It should be noted that Robert's results use an extra move for his version of Kirby Calculus here denoted as \mathcal{O}_3 . We show that the three manifolds that we construct can be chosen to have associated four manifolds that are simply connected, and that in this category, the topological types of these three manifolds are classified by just the first two of the moves \mathcal{O}_1 (Figure 4.1) and \mathcal{O}_2 (Figure 4.2). Restricting ourselves to this category of three-manifolds, the first two moves correspond to the classical Kirby Calculus and to the generalized Kirby Calculus for virtual diagrams.

The \mathcal{O}_1 and \mathcal{O}_2 moves do not change the Dye-Kauffman quantum invariants ς_r for framed virtual links. When Kauffman and Ogasa wrote the paper [14], it was open whether the \mathcal{O}_3 move changes the Dye-Kauffman quantum invariants ς_r . Kauffman and Ogasa avoided the \mathcal{O}_3 move in order to introduce a topological invariant. Kauffman and Ogasa [14] introduced a condition, *the simple connectivity condition*, succeeded to avoid the \mathcal{O}_3 move difficulty, and defined the new quantum invariants ν_r (see §5).

In this paper we proved the following about the above question.

Remark 11.3. *In general, the \mathcal{O}_3 move on framed virtual links changes the Dye-Kauffman quantum invariants ς_r for framed virtual links.*

Remark 11.3 implies the following.

Remark 11.4. *In Definition 9.1, the simple connectivity condition is necessary to define the our quantum invariants ν_r .*

Note that we work only with closed oriented 3-manifolds that bound specific simply connected compact 4-manifolds, usually with these 4-manifolds corresponding to surgery instructions on a given link. Thus we concentrate on framed links that represent given 3-manifolds with boundary and that represent simply connected 4-manifolds.

In this way, we are able to apply Robert's results and make the connection between the topological types in a category of three manifolds and the Kirby Calculus classes of virtual link diagrams. With these connections in place, the paper ends with a description of the construction of the Witten-Reshetikhin-Turaev invariants τ_r that apply, via virtual Kirby Calculus, to our category of three-manifolds. We obtain our new invariant v_r .

We examine links that are embedded in thickened surfaces and obtain new invariants v_r of three manifolds obtained by surgery on these thickened surfaces. One could take the viewpoint that the thickened surfaces are embedded in the three sphere and so also consider the three manifolds obtained by surgery on the links in the three sphere. These two points of view are distinct and give distinct invariants. This point of view for links in thickened surfaces is distinct from the usual point of view for the Reshetikhin Turaev invariants τ_r , and our invariants v_r give distinct results from these invariants. See §14.

The invariants τ_r are defined only for framed classical links. If L^{fr} is a framed classical link, the three invariants, τ_r , ς_r , and v_r , for L^{fr} are equal. The two invariants, ς_r and v_r are defined for all framed virtual links. The invariants v_r have different properties from the invariants ς_r . It is a main theme of this paper.

As written above, the Dye-Kauffman invariants ς_r of framed virtual links do not produce a topological invariant of 3-manifolds if we do not impose the simple connectivity condition. In this paper we put an emphasis on this fact and we say that the Reshetikhin-Turaev invariants τ_r and our invariants v_r are topological quantum invariants although we usually just say quantum invariants.

Part 1. The new quantum invariants v_r : Review of the definition

2. Quantum invariants v_r of 3-manifolds with boundary

Definition 2.1. Let M be a connected compact oriented 3-manifold with boundary. Let $\partial M = G \amalg H$, where G and $-H$ are both orientation preserving diffeomorphic to a given closed oriented surface F with genus g . Fix a symplectic basis m_1^G, \dots, m_g^G , (respectively, m_1^H, \dots, m_g^H), and longitudes, l_1^G, \dots, l_g^G , (respectively, l_1^H, \dots, l_g^H), for G (respectively, H) as usual. That is, the cohomology products of two basis elements are as follows: $m_i^G \cdot l_i^G = +1$. $l_i^G \cdot m_i^G = -1$. The others are zero.

Under these conditions, the 3-manifold M is said to satisfy *boundary condition* \mathcal{B} .

We sometimes write $-F$ (respectively, $F \amalg -F$) as F (respectively, $F \amalg F$) when it is clear from the context.

We shall define topological quantum invariants of 3-manifolds M with boundary condition \mathcal{B} below.

Remark: For an oriented manifold X , we sometimes write $-X$ as X when it is clear from the context.

3. Framed links in thickened surfaces

It is well-known that we can define the linking number for 2-component links in \mathbb{R}^3 . On the other hand, in general, we cannot define it in the case of compact oriented 3-manifolds. However, we can define it in the case of thickened surfaces as below.

Definition 3.1. Let (J, K) be a link in a thickened surface $F \times [-1, 1]$, where J and K may be non-zero 1-cycles. We define the *linking number* $\text{lk}(J, K)$ of J and K as follows. Let Z stand for either J or K . The knot Z together with a collection of circles in $F \times \{-1\}$ bounds a compact oriented surface M_Z in $F \times [-1, 1]$. Assume that J (respectively, K) intersects M_K (respectively, M_J) transversely. Let $I(J, M_K)$ (respectively, $I(K, M_J)$) be the algebraic intersection number of J and M_K (respectively, K and M_J). Note that $I(J, M_K) \neq I(K, M_J)$ in general. Let $\text{lk}(J, K)$ be
$$\frac{1}{2}\{I(J, M_K) + I(K, M_J)\}.$$

This is well-defined. It is proved by Reidemeister moves.

Remark 3.2. (1) The linking number $\text{lk}(J, K)$ of a link (J, K) in a thickened surface may be a half integer. Figure 3.1 draws an example: The linking number of this link is $\frac{1}{2}$. The places where a circle (inner and outer circles in the depiction of the torus surface) is cut indicate how the curves go from the upper part of the torus to the lower part (with respect to the projection directions chosen for this drawing). This discrimination allows us to indicate which crossings of the curves are actual weavings and which (dotted to solid curves) are artifacts of the projection.

If F is the 2-sphere, then $I(J, M_K) = I(K, M_J)$ holds and $\text{lk}(J, K)$ is an integer.

(2) If F is the 2-sphere, embed $F \times [-1, 1]$ in the 3-sphere naturally. Regard a link (J, K) in the thickened 2-sphere as a link in the 3-sphere. Then the well-known linking number of the link (J, K) in the 3-sphere is equal to the linking number $\text{lk}(J, K)$ in Definition 3.1.

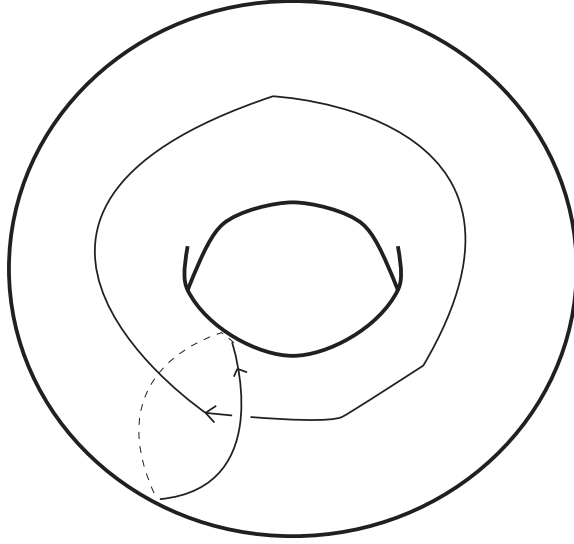


FIGURE 3.1. A link in the thickened torus. The linking number is $\frac{1}{2}$.

An equivalent way to define linking numbers of links in thickened surfaces is as follows.

Definition 3.3. Let (J, K) be a link in $F \times [-1, 1]$. Make a projection of (J, K) into $F \times \{-1\}$. Assume that the projection map is a self-transverse immersion. Just as we can take a diagram of a classical link in the plane, we can use such diagrams, which is the projection, in the surface $F \times \{-1\}$. We give each crossing point of J and K $+1$ or -1 by using the orientation of J , that of K , and that of $F \times \{-1\}$. The *linking number* $\text{lk}(J, K)$ is the half of the sum of the numbers at all crossing points.

This is well-defined. It is proved by Reidemeister moves. The equivalence between two definitions above is also proved by Reidemeister moves.

Framings. Let K be a knot in a compact oriented 3-manifold M . Recall that, in this paper, for a link L in M , $N(L)$ is the total space of the open D^2 -bundle over L . Let $\overline{N(K)}$ be the closure of the tubular neighborhood of K in M . Take a knot J in $\partial(\overline{N(K)})$ so that J is homotopic to K in $\overline{N(K)}$. We cannot define the linking number of K and J in general. If M is a thickened surface, the linking number of K and J makes sense (Recall Definitions 3.1 and 3.3). Then it is an integer, not a half integer.

Remark 3.4. For any 3-manifold M , we can always specify attaching maps of 4-dimensional 2-handles to M by using a chart of M . However, we cannot determine the map by just choosing an integer for framing. The integer needs to be interpreted as a linking number of a curve on the boundary of a tubular neighborhood with the core of the solid torus. For this, it does suffice to have the surgeries on manifolds M of type $F \times [-1, 1]$ where F is a surface.

Let K be a knot in a compact oriented 3-manifold M . Let $D^2 \times B^2$ denote a 4-dimensional 2-handle such that $D^2 \times \partial B^2$ is the attaching part. Let O be the center of D^2 , and P a point in ∂D^2 . We attach a 4-dimensional 2-handle $D^2 \times B^2$ along a knot K in M so that $O \times \partial B^2$ coincides with K . Then $(O \times \partial B^2, P \times \partial B^2)$ is a 2-component link in M . When we want to introduce framings associated with attaching 4-dimensional 2-handles, we have to note the following fact. We cannot define the linking number of $O \times \partial B^2$ and $P \times \partial B^2$ in M in general. Therefore framings do not make sense in general. If M is a thickened surface, framings make sense, and are always integers.

Definition 3.5. A *framed link* L^{fr} in a thickened surface is a link $L = (K_1, \dots, K_n)$ in a thickened surface such that each component K_i is equipped with an integer in the sense described above so that this integer is a linking number. The integer is called the *framing* for K_i .

Note that framings are always integers.

Assume that a component K of framed link L^{fr} in a thickened surface has a framing n . Take $\overline{N(K)}$ of K in the thickened surface. Embed a circle C in $\partial(\overline{N(K)})$ which is homotopic to K in $\overline{N(K)}$ so that $\text{lk}(K, C) = n$. We attach a 4-dimensional 2-handle $D^2 \times B^2$ along a knot K so that $O \times \partial B^2$ coincides with K and so that $P \times \partial B^2$ coincides with C .

Thus L^{fr} represents, via framed surgery, a compact oriented 3-manifold with boundary whose boundary is a disjoint union of the same two surfaces $F \amalg -F$. It also represents a 4-manifold.

See Figure 3.2 for an example. A framed link embedded in a thickened surface is drawn as a framed link in the surface which is the projection of a thickened surface. Recall the explanation of drawing diagrams in Remark 3.2.(1).

Definition 3.6. Define $F \times [-1, 1]$ with *the symplectic basis condition* \mathcal{F} as follows.

Take $F \times [-1, 1]$. Fix a symplectic basis, m_1^F, \dots, m_g^F , and l_1^F, \dots, l_g^F , for F as usual.

Fix $m_i^F \times \{+1\}$ and $l_i^F \times \{+1\}$ (respectively, $m_i^F \times \{-1\}$ and $l_i^F \times \{-1\}$) in $F \times \{+1\}$ (respectively, $F \times \{-1\}$).

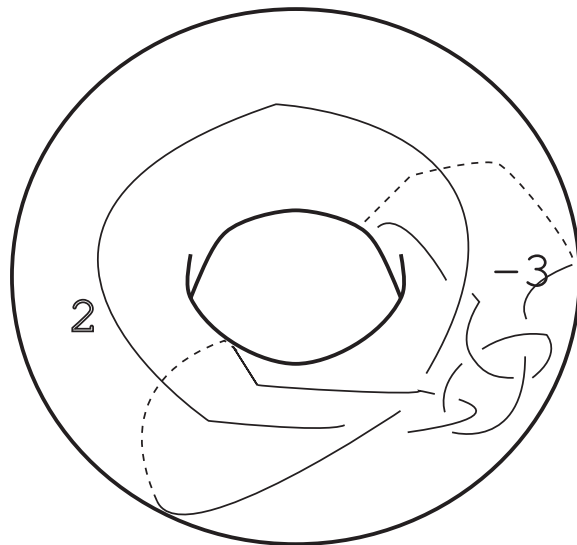


FIGURE 3.2. A framed link in the thickened torus

A framed link L^{fr} in $F \times [-1, 1]$ with the symplectic basis condition \mathcal{F} represents a compact oriented 3-manifold with the boundary $F \amalg F$ with the boundary condition \mathcal{B} . It also represents a 4-manifold.

Remark: Note that another equivalent way to obtain framed links for the purpose of doing surgery on $F \times I$ is to use a generalized blackboard framing for a diagram drawn in the surface F . Just as we can take a diagram of a classical link in the plane and regard it as a framed link by not using the first Reidemeister move and regarding the diagram itself as specifying a framing [12], we can use such diagrams in the surface F . In fact we can start with such a blackboard framed virtual link diagram (See §7), take the corresponding standard (abstract link diagram) construction producing a link diagram L in a surface F . The blackboard framing on the virtual diagram then induces a blackboard framing on the diagram in the surface. We will use this association to show how the quantum link invariants we have previously defined for virtual link diagrams [4] become quantum invariants of actual three-manifolds via the constructions in this paper.

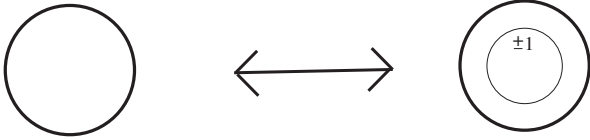


FIGURE 4.1. The operation \mathcal{O}_1 in the 3-ball

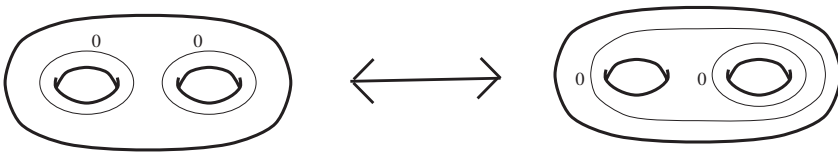


FIGURE 4.2. The operation \mathcal{O}_2 in the genus two handle-body

Virtual links are represented by links in thickened surfaces. We use these properties and define our quantum invariants.

4. Framed link representations of 3-manifolds with non-vacuous boundary

Roberts [35] generalized the result of Kirby[18] and the result of Fenn and Rourke[5], and proved a theorem that is stronger than Theorem 4.1 below.

Theorem 4.1. (This Theorem follows from Roberts' result [35]) *Let F be a closed oriented surface. Let M be a compact oriented 3-manifold with boundary, whose boundary is $F \amalg F$, with the boundary condition \mathcal{B} . Let L_0 and L_1 be framed links in $F \times [-1, 1]$ with the symplectic basis condition \mathcal{F} , which represent M .*

Then L_0 and L_1 are related by the moves \mathcal{O}_1 in Figure 4.1, \mathcal{O}_2 in Figure 4.2, \mathcal{O}_3 in Figure 4.3, and framed isotopy in $F \times [-1, 1]$.

Remark: The \mathcal{O}_1 move is carried out in the 3-ball (Figure 4.1). The \mathcal{O}_2 move is carried out in the genus two handle-body (Figure 4.2). The \mathcal{O}_3 move is carried out in the solid torus, not the thickened torus. (Figure 4.3).

5. Framed links in thickened surfaces and simply connected 4-manifolds

We prove Theorem 5.2 below, which is different from Theorem 4.1. This difference is very important. We use Theorem 5.2 and define our topological quantum invariant.

Definition 5.1. If a framed link L^{fr} in $F \times [-1, 1]$ represents a simply connected 4-manifold V , we call L^{fr} a framed link with *the simple-connectivity condition \mathcal{S}* .

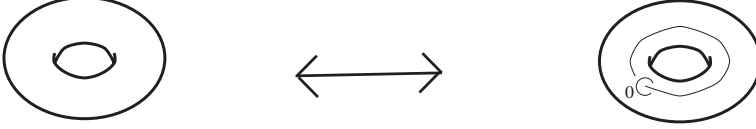


FIGURE 4.3. The operation \mathcal{O}_3 in the solid torus

By [35], we have the following.

Theorem 5.2. *Let M be a connected compact oriented 3-manifold with the boundary $F \amalg F$ with the boundary condition \mathcal{B} (in Definition 2.1). Then M is always described by a framed link in $F \times [-1, 1]$ with the symplectic basis condition \mathcal{F} (in Definition 3.6) and with the simple-connectivity condition \mathcal{S} (in Definition 5.1).*

Proof of Theorem 5.2. Take a framed link L^{fr} which represents V . Use the operation \mathcal{O}_3 in Figure 4.3, finitely many times, as shown in Figure 5.1: Add a framed link to L^{fr} as drawn in Figure 5.1. Recall the explanation of drawing diagrams in Remark 3.2.(1).

An example is drawn in Figure 5.2. \square

We have also proved the following now.

Theorem 5.3. *Let L^{fr} be a framed link $F \times [-1, 1]$ with the symplectic basis condition \mathcal{F} (in Definition 3.6).*

Suppose that L^{fr} represents a connected compact oriented 3-manifold with the boundary $F \amalg F$ with the boundary condition \mathcal{B} (in Definition 2.1).

Then there is an explicit way to make the given framed link L^{fr} into a framed link A^{fr} in $F \times [-1, 1]$ with the symplectic basis condition \mathcal{F} and with the simple-connectivity condition \mathcal{S} . Furthermore, L^{fr} is a sub-framed link of A^{fr} .

We generalize the results in Kirby, Fenn and Rourke, and Roberts [5, 18, 35], and we prove the following.

Theorem 5.4. *Let F be a connected closed oriented surface. Let M be a connected oriented compact 3-manifold with boundary $F \amalg F$ with the boundary condition \mathcal{B} . Let L^{fr} and $L^{fr'}$ be framed links in $F \times [-1, 1]$ with the symplectic basis condition \mathcal{F} and with the simple-connectivity condition \mathcal{S} , that represent M . Then L^{fr} is made from $L^{fr'}$ by a finite sequence of handle-slide, adding and removing the disjoint trivial knots with framing ± 1 , that is, Kirby moves ([20]). Note that under the hypothesis of this theorem we only use Roberts moves \mathcal{O}_1 and \mathcal{O}_2 .*

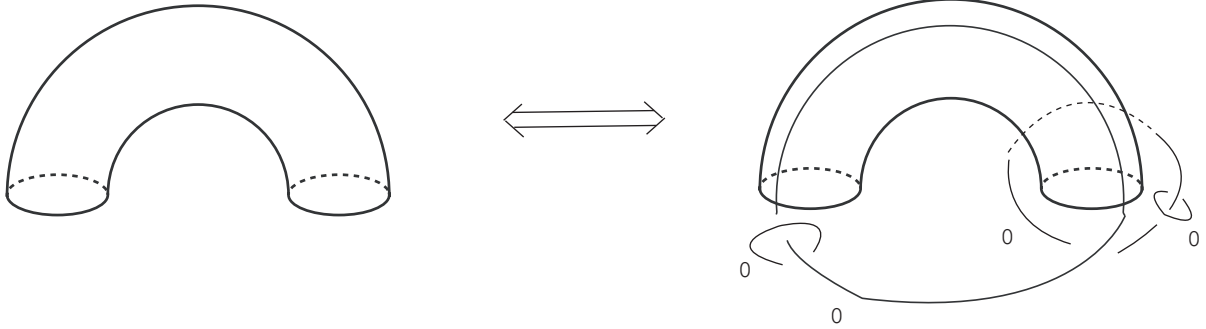


FIGURE 5.1. Two times of the \mathcal{O}_3 moves

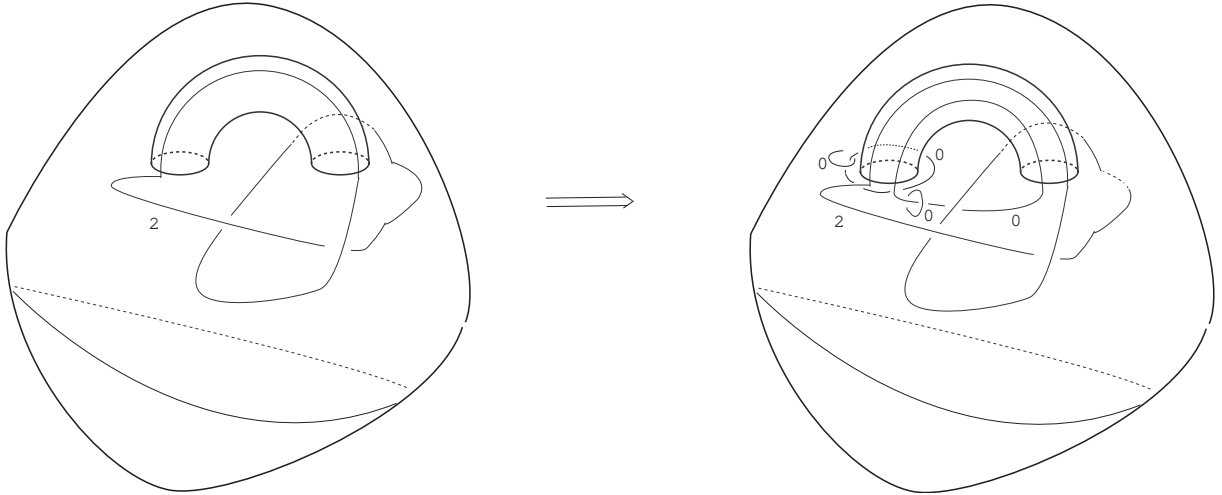


FIGURE 5.2. Adding a framed link produces a new framed link with the simple-connectivity condition \mathcal{S}

Under these assumptions we have four manifolds V and V' as described in Definition 5.1. Then

$V \sharp^\alpha (S^2 \times S^2) \sharp^\beta (S^2 \tilde{\times} S^2) \sharp^\gamma \overline{CP^2 \sharp^\delta CP^2}$ is diffeomorphic to $V' \sharp^{\alpha'} (S^2 \times S^2) \sharp^{\beta'} (S^2 \tilde{\times} S^2) \sharp^{\gamma'} \overline{CP^2 \sharp^{\delta'} CP^2}$, where $\alpha, \beta, \gamma, \delta, \alpha', \beta', \gamma'$ and δ' are non-negative integers.

Remark 5.5. Kirby moves mean the only \mathcal{O}_1 and \mathcal{O}_2 moves.

If we do not impose the simple-connectivity condition \mathcal{S} in Theorem 5.4, L^{fr} is not made from $L^{fr'}$ by a finite sequence of Kirby moves in general. See Figure 5.3. Recall the explanation of drawing diagrams in Remark 3.2.(1). In the right figure of Figure 5.3, we

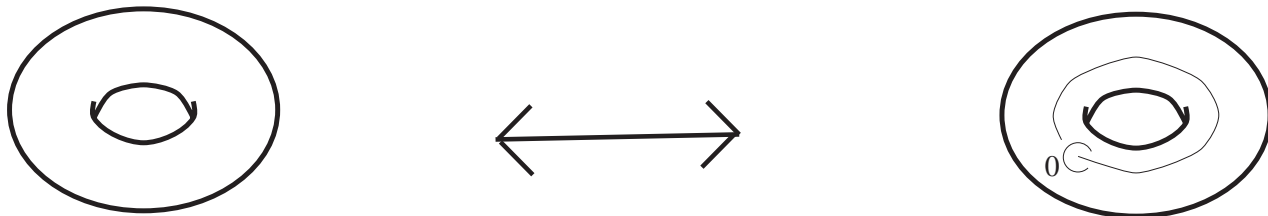


FIGURE 5.3. Two framed links in the thickened torus

draw a framed link in the torus which is the projection of the thickened torus. The place where a circle is cut means which segments there goes over or down, as usual. The left figure of Figure 5.3 represents the empty framed link. The two framed links represent the same 3-manifold, but they are not Kirby move equivalent. Note the difference between Figures 4.3 and 5.3. In Figure 4.3, we drew the solid torus.

The simple connectivity condition is important. Under the simple connectivity condition of framed links, we can carry out the \mathcal{O}_3 move by using the \mathcal{O}_1 and \mathcal{O}_2 moves. Figure 5.4 is an example.

6. Quantum invariants ζ_r of framed virtual links: Outline

Kauffman [8, 10, 11] describes and develops virtual links as a diagrammatic extension of classical links, and as a representation of links embedded in thickened surfaces. The Jones polynomial of virtual links is defined in [8, 10, 11]. See related open questions in [32, §4].

We can regard any framed link in $F \times [-1, 1]$ as a framed virtual link. See [4] for framed virtual links. Note that the linking number of any pair, K_i and K_j , is defined. The value is an integer or a half integer. Note that the framing is an integer.

Dye and Kauffman defined quantum invariants ζ_r of framed virtual links (See §8). If two framed links L^{fr} and $L^{fr'}$ are changed into each other by a sequence of Kirby moves ([20]) and classical and virtual Reidemeister moves, each of the Dye-Kauffman quantum invariants ζ_r of L^{fr} is equivalent to that of $L^{fr'}$.

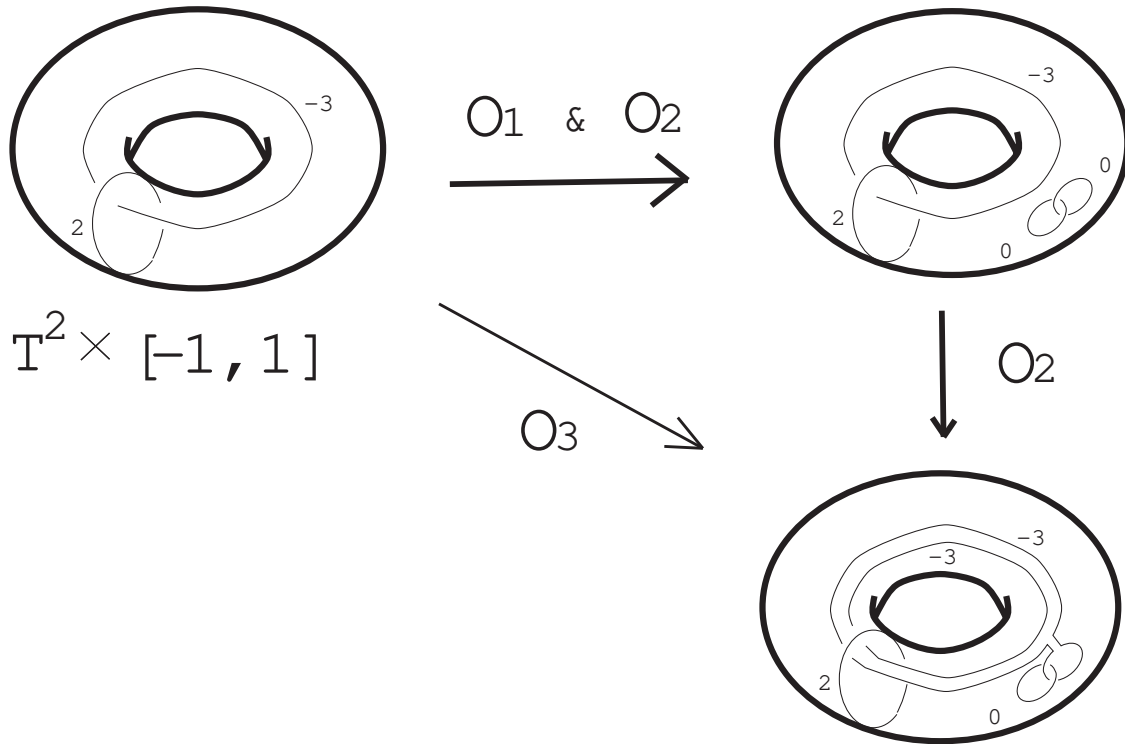


FIGURE 5.4. An \mathcal{O}_3 move realized by \mathcal{O}_1 and \mathcal{O}_2 moves under the simple connectivity condition

We use these invariants ς_r and, introduce quantum invariants v_r of 3-manifolds with boundary in the following sections.

7. Virtual knots and virtual links

The theory of *virtual knots* ([8, 10, 11]) is a generalization of classical knot theory, and studies the embeddings of circles in thickened oriented closed surfaces modulo isotopies and orientation preserving diffeomorphisms plus one-handle stabilization of the surfaces.

By a one-handle stabilization, we mean a surgery on the surface that is performed on a curve in the complement of the link embedding and that either increases or decreases the genus of the surface. The reader should note that knots and links in thickened surfaces can be represented by diagrams on the surface in the same sense as link diagrams drawn in the plane or on the two-sphere. From this point of view, a one handle stabilization is obtained by cutting the surface along a curve in the complement of the link diagram and capping the two new boundary curves with disks, or taking two points on the surface

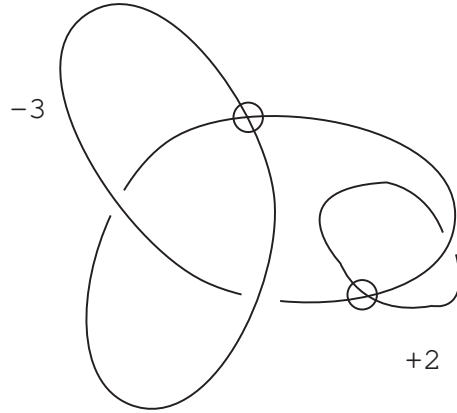


FIGURE 6.1. A framed virtual link

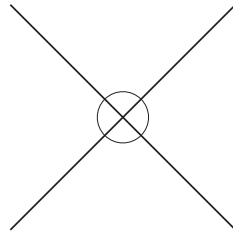


FIGURE 7.1. Virtual crossing point

in the link diagram complement and cutting out two disks, and then adding a tube between them. The main point about handle stabilization is that it allows the virtual knot to be eventually placed in a least genus surface in which it can be represented. A theorem of Kuperberg [21] asserts that such minimal representations are topologically unique.

Virtual knot theory has a diagrammatic formulation. A *virtual knot* can be represented by a *virtual knot diagram* in \mathbb{R}^2 (respectively, S^2) containing a finite number of real crossings, and *virtual crossings* indicated by a small circle placed around the crossing point as shown in Figure 7.1. A virtual crossing is neither an over-crossing nor an under-crossing. A virtual crossing is a combinatorial structure keeping the information of the arcs of embedding going around the handles of the thickened surface in the surface representation of the virtual link.

The moves on virtual knot diagrams in \mathbb{R}^2 are generated by the usual Reidemeister moves plus the *detour move*. The detour move allows a segment with a consecutive sequence of virtual crossings to be excised and replaced by any other such a segment with

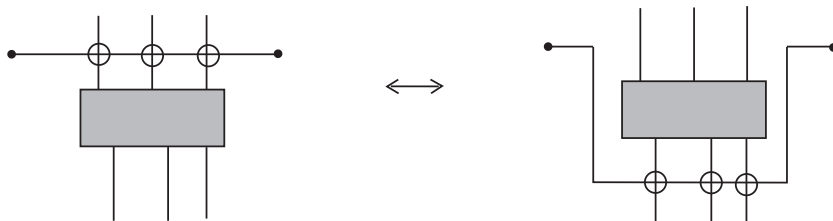


FIGURE 7.2. An example of detour moves

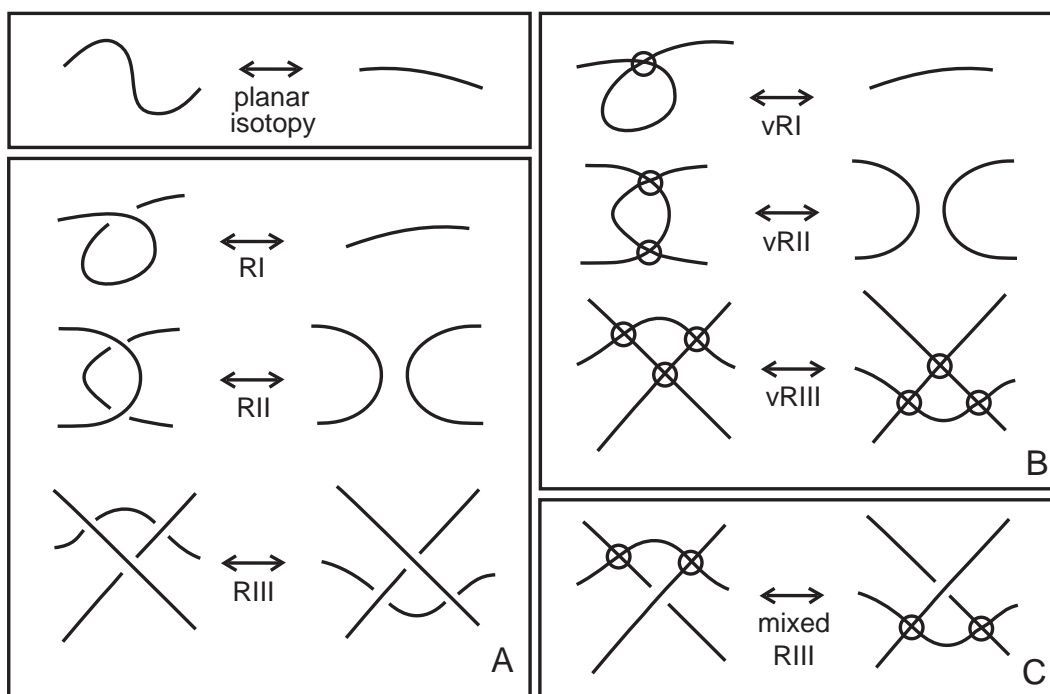


FIGURE 7.3. All Reidemeister moves

a consecutive virtual crossings, as shown in Figure 7.2.

Virtual 1-knot diagrams α and β are changed into each other by a sequence of the usual Reidemeister moves and detour moves if and only if α and β are changed into each other by a sequence of all Reidemeister moves drawn in Figure 7.3.

Virtual knot and link diagrams that can be related to each other by a finite sequence of the Reidemeister and detour moves are said to be *virtually equivalent* or *virtually isotopic*.

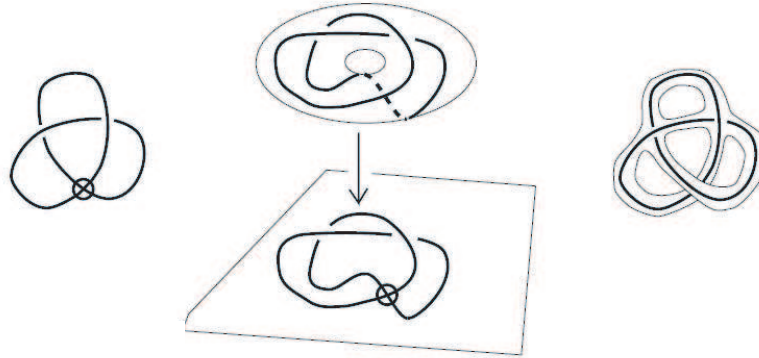


FIGURE 7.4. How to make a representing surface from the tubular neighborhood of a virtual knot diagram in \mathbb{R}^2

The virtual isotopy class of a virtual knot diagram is called a *virtual knot*.

There is a one-to-one correspondence between the topological and the diagrammatic approach to virtual knot theory. The following theorem providing the transition between the two approaches is proved by abstract knot diagrams, see [8, 10, 11].

Theorem 7.1. ([8, 10, 11]) *Two virtual link diagrams are virtually isotopic if and only if their surface embeddings are equivalent up to isotopy in the thickened surfaces, orientation preserving diffeomorphisms of the surfaces, and the addition/removal of empty handles.*

Remark: A handle is said to be *empty* if the knot diagram does not thread through the handle. One way to say this more precisely is to model the addition of and removal of handles via the location of surgery curves in the surface that do not intersect the knot diagram. Here, an oriented surface with a link diagram using only classical crossings appears. This surface is called a *representing surface*. In many figures of this paper, we use representing surfaces.

In Figure 7.4 we show an example of a way to make a representing surface from a virtual knot diagram. Take the tubular neighborhood of a virtual knot diagram in \mathbb{R}^2 . Near a virtual crossing point, double the tubular neighborhood. Near a classical crossing point, keep the tubular neighborhood and the classical crossing point. Thus we obtain a compact representing surface with non-vacuous boundary. We may start with a representing surface that is oriented and not closed, and then embed the surface in a closed oriented surface to obtain a new representing surface. Taking representations of virtual knots up to such cutting (removal of exterior of neighborhood of the diagram in a given surface) and re-embedding, plus isotopy in the given surfaces, corresponds to a unique diagrammatic virtual knot type.

The linking number.

Recall the linking number of links in thickened surfaces in Definitions 3.1 and 3.3. If a link (J, K) in $F \times [-1, 1]$ is virtually equivalent to a link (J', K') in $F' \times [-1, 1]$, then we have $\text{lk}(J, K) = \text{lk}(J', K')$. Therefore the following definition makes sense.

Definition 7.2. Let $(\mathcal{J}, \mathcal{K})$ be a virtual link represented by a link (J, K) in $F \times [-1, 1]$. Define the *linking number* $\text{lk}(\mathcal{J}, \mathcal{K})$ to be $\text{lk}(J, K)$.

We have an alternative definition as below.

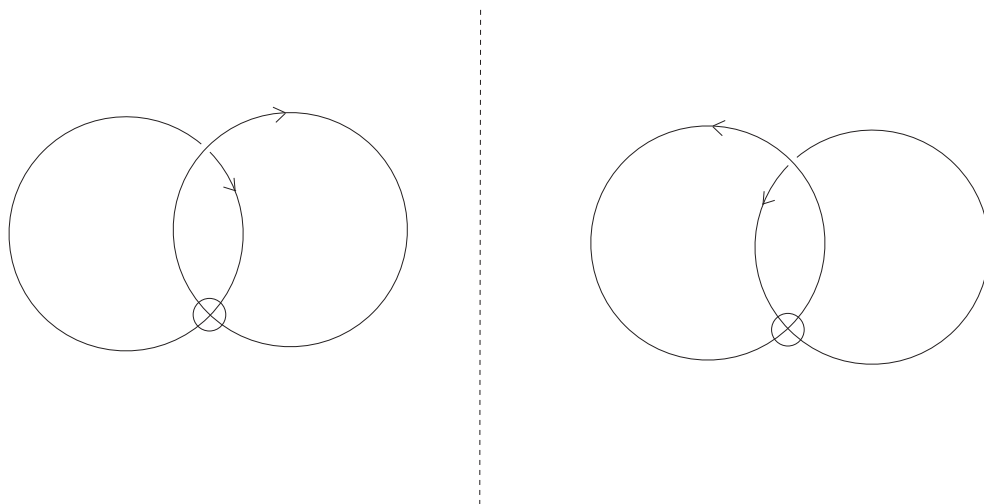
Definition 7.3. Let (P, Q) be a virtual link diagram which represents a virtual link $(\mathcal{P}, \mathcal{Q})$. Each classical crossing point of P and Q is oriented by the orientation of P , that of Q and that of the plane. Assign to a positive classical crossing (respectively, a negative classical crossing, a virtual crossing) $+1$ (respectively, $-1, 0$). Define $\text{lk}(P, Q)$ to be the half of the sum of the number associated with each crossing point. Define the *linking number* $\text{lk}(\mathcal{P}, \mathcal{Q})$ to be $\text{lk}(P, Q)$.

Examples are drawn in Figure 7.5. The linking number of the left virtual link is $-\frac{1}{2}$. The linking number of the right virtual link is $\frac{1}{2}$.

Manturov's textbook [29] and its English translation [6] by Ilyutko and Manturov are introduction to virtual knot theory.

8. Quantum invariants ς_r of framed virtual links: Review of Definition

Dye and Kauffman [4] extended the definition of the Witten-Reshetikhin-Turaev invariant τ_r [33, 34, 40] to virtual link diagrams, and defined the Dye-Kauffman quantum invariants ς_r of framed virtual links. In this section $Z_K(r)$ denotes ς_r and we review the definition. See [4] for detail.

FIGURE 7.5. **Virtual Hopf link**

First, we recall the definition of the Jones-Wenzl projector (q-symmetrizer) [12]. We then define the colored Jones polynomial of a virtual link diagram. It is clear from this definition that two equivalent virtual knot diagrams have the same colored Jones polynomial. We use these definitions to extend the Witten-Reshetikhin-Turaev invariant τ_r to virtual link diagrams. From this construction, we conclude that two virtual link diagrams, related by a sequence of framed Reidemeister moves and virtual Reidemeister moves, have the same value of the generalization ς_r of the Witten-Reshetikhin-Turaev invariant τ_r . Finally, we prove that the generalization ς_r of the Witten-Reshetikhin-Turaev invariant τ_r is unchanged by the virtual Kirby calculus.

To form the n -cabling of a virtual knot diagram, take n parallel copies of the virtual knot diagram. A single classical crossing becomes a pattern of n^2 classical crossings and a single virtual crossing becomes n^2 virtual crossings.

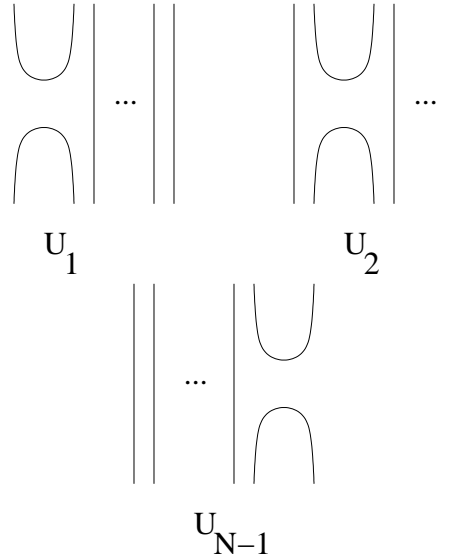
Let r be a fixed integer such that $r \geq 2$ and let

$$A = e^{\frac{\pi i}{2r}}.$$

Here is a formula used in the construction of the Jones-Wenzl projector.

$$\Delta_n = (-1)^n \frac{A^{2n+2} - A^{-(2n+2)}}{A^2 - A^{-2}}.$$

Note that $\Delta_1 = -(A^2 + A^{-2})$, the value assigned to a simple closed curve by the bracket polynomial. There will be an analogous interpretation of Δ_n which we will discuss

FIGURE 8.1. Tangles U_i

later in this section.

We recall the definition of an n -tangle. Any two n -tangles can be multiplied by attaching the bottom n strands of one n -tangle to the upper n strands of another n -tangle. We define an n -tangle to be *elementary* if it contains no classical or virtual crossings. Note that the product of any two elementary tangles is elementary. Let I denote the identity n -tangle and let U_i such that $i \in \{1, 2, \dots, n-1\}$ denote the n -tangles shown in Figure 8.1.

By multiplying a finite set of U_* as in $U_{i_1}U_{i_2}\dots U_{i_n}$, we can obtain any elementary n -tangle. Formal sums of the elementary tangles over $\mathbb{Z}[A, A^{-1}]$ generate the n^{th} Temperley-Lieb algebra [12].

We recall that the n^{th} Jones-Wenzl projector is a certain sum of all elementary n -tangles with coefficients in \mathbb{C} [9, 12]. We denote the n^{th} Jones-Wenzl projector as T_n . We indicate the presence of the Jones-Wenzl projector and the n -cabling by labeling the component of the knot diagram with n .

Remark 8.1. There are different methods of indicating the presence of a Jones-Wenzl projector. In a virtual knot diagram, the presence of the n^{th} Jones-Wenzl projector is indicated by a box with n strands entering and n strands leaving the box. For n -cabled components of a virtual link diagram with an attached Jones-Wenzl projector, we indicate

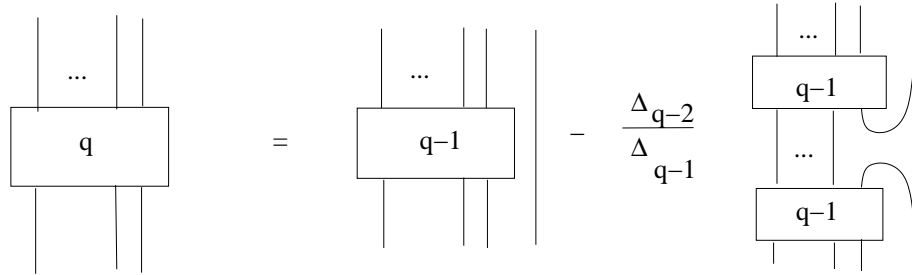


FIGURE 8.2. q^{th} Jones-Wenzl Projector

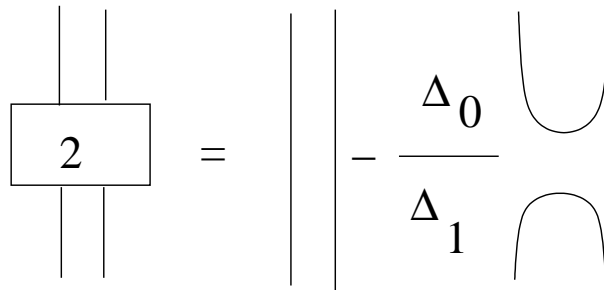


FIGURE 8.3. 2^{nd} Jones-Wenzl Projector

the cabling by labeling the component with n and the presence of the projector with a box. This notation can be simplified to the convention indicated in the definition of the colored Jones polynomial. The choice of notation is dependent on the context.

We construct the Jones-Wenzl projector recursively. The 1^{st} Jones-Wenzl projector consists of a single strand with coefficient 1. There is exactly one 1-tangle with no classical or virtual crossings. The q^{th} Jones-Wenzl projector is constructed from the $(q - 1)^{th}$ and $(q - 2)^{th}$ Jones-Wenzl projectors as illustrated in figure 8.2.

We use this recursion to construct the 2^{nd} Jones-Wenzl projector as shown in figure 8.3.

We will refer to the Jones-Wenzl projector as the J-W projector for the remainder of this paper.

We review the properties of the J-W projector. Recall that if T_n denotes the n^{th} J-W projector then

i) $T_n T_m = T_n$ for $n \geq m$,

ii) $T_n U_i = 0$ for all i ,

iii) The bracket evaluation of the closure of $T_n = \Delta_n$.

Remark 8.2. The combinatorial definition of the J-W projector is given in [12], p. 15. Note that [12] provides a full discussion of all formulas given above.

Let K be a virtual link diagram with components $K_1, K_2 \dots K_n$. Fix an integer $r \geq 2$ and let $a_1, a_2 \dots a_n \in \{0, 1, 2, \dots, r-2\}$. Let \bar{a} represent the vector (a_1, a_2, \dots, a_n) . Fix $A = e^{\frac{\pi i}{2r}}$ and $d = -A^2 - A^{-2}$. We denote the *generalized \bar{a} colored Jones polynomial* of K as $\langle K^{\bar{a}} \rangle$. To compute $\langle K^{\bar{a}} \rangle$, we cable the component K_i with a_i strands and attach the a_i^{th} J-W projector to cabled component K_i . We apply the Jones polynomial to the cabled diagram with attached J-W projectors.

The colored Jones polynomial is invariant under the framed Reidemeister moves and the virtual Reidemeister moves. This result is immediate, since the Jones polynomial is invariant under the framed Reidemeister moves and the virtual Reidemeister moves.

Remark 8.3. The a -colored Jones polynomial of the unknot is Δ_a . In other words, the Jones polynomial of the closure of the a^{th} J-W projector is Δ_a .

The *generalized Witten-Reshetikhin-Turaev invariant* of a virtual link diagram is a sum of colored Jones polynomials. Let K be a virtual knot diagram with n components. Fix an integer $r \geq 2$. We denote the unnormalized Witten-Reshetikhin Turaev invariant of K as $\langle K^\omega \rangle$, which is shorthand for the following equation.

$$(8.1) \quad \langle K^\omega \rangle = \sum_{\bar{a} \in \{0,1,2,\dots,r-2\}^n} \Delta_{a_1} \Delta_{a_2} \dots \Delta_{a_n} \langle K^{\bar{a}} \rangle$$

Remark 8.4. For the remainder of this paper, the Witten-Reshetikhin-Turaev invariant τ_r will be referred to as the WRT.

We define the matrix N in order to construct the normalized WRT [12]. Let N be the matrix defined as follows:

i) $N_{ij} = lk(K_i, K_j)$ for $i \neq j$,

ii) $N_{ii} = w(K_i)$.

Then let

$b_+(K) =$ the number of positive eigenvalues of N ,

$b_-(K) =$ the number of negative eigenvalues of N ,

and

$n(k) = b_+(K) - b_-(K)$.

The *normalized WRT* of a virtual link diagram K is denoted as $Z_K(r)$. (This is the Dye-Kauffman quantum invariant ς_r . See Remark 11.2. The Dye-Kauffman quantum invariants ς_r are defined only for framed virtual links. It is not defined for 3-manifolds. Kauffman and Ogasa [14] used the Dye-Kauffman quantum invariants ς_r , and introduced new topological quantum invariants v_r for 3-manifolds.)

Let $A = e^{\frac{\pi i}{2r}}$ and let $|k|$ denote the number of components in the virtual link diagram K . Then $Z_K(r)$ is defined by the formula

$$Z_K(r) = \langle K^\omega \rangle \mu^{|K|+1} \alpha^{-n(K)}$$

where

$$\mu = \sqrt{\frac{2}{r}} \sin\left(\frac{\pi}{r}\right)$$

and

$$\alpha = (-i)^{r-2} e^{i\pi[\frac{3(r-2)}{4r}]}$$

This normalization is chosen so that normalized WRT of the unknot with writhe zero is 1 and the normalization is invariant under the introduction and deletion of ± 1 framed unknots.

Let \hat{U} be a $+1$ framed unknot. We recall that $\alpha = \mu \langle \hat{U}^\omega \rangle$ [12], page 146. Since \hat{U} and K are disjoint in $K \amalg \hat{U}$ then $\langle (K \amalg \hat{U})^\omega \rangle = \langle K^\omega \rangle \langle \hat{U}^\omega \rangle$. We note that $b_+(K \amalg \hat{U}) = b_+(K) + 1$, $b_-(K \amalg \hat{U}) = b_-(K)$, and $|K \amalg \hat{U}| = |K| + 1$. We compute that

$$Z_{K \amalg \hat{U}}(r) = \langle K^\omega \rangle \langle \hat{U}^\omega \rangle \mu^{|K|+2} \alpha^{-n(K)-1}.$$

As a result,

$$Z_{K \amalg \hat{U}}(r) = Z_K(r).$$

Theorem 8.5. *Let K be a virtual link diagram then $Z_K(r)$ or ς_r is invariant under the framed Reidemeister moves, virtual Reidemeister moves, and the virtual Kirby calculus.*

Remark: The virtual Kirby calculus means a sequence of only the \mathcal{O}_1 and \mathcal{O}_2 moves. Theorem 8.5 never answers whether the \mathcal{O}_3 move changes the Dye-Kauffman invariants ς_r or not. Kauffman and Ogasa [14] avoided answering this question, and succeeded to introduce new topological invariants v_r by using the Dye-Kauffman invariants ς_r . We review it in the following section §9.

Furthermore, we prove in Proposition 11.1 that the \mathcal{O}_3 move changes the Dye-Kauffman invariants ς_r in general.

9. Our topological quantum invariants v_r of 3-manifolds with boundary

Definition 9.1. Let F be a connected closed oriented surface. Let M be a connected oriented compact 3-manifold with the boundary $F \amalg F$ with the boundary condition \mathcal{B} . Let L^{fr} in $F \times [-1, 1]$ with the symplectic basis condition \mathcal{F} be a framed link with the simple-connectivity condition \mathcal{S} which represents M . Regard L^{fr} as a framed virtual link. Define our *quantum invariants* v_r of M to be the Dye-Kauffman quantum invariants ζ_r of the framed virtual link.

By Theorem 5.4 and §6, we have the following.

Main Theorem 9.2. *Definition 9.1 is well-defined, that is, each of the quantum invariants v_r of M is a topological invariant.*

Remark 9.3. Take a framed link in $F \times I$ with the symplectic basis condition. The value, $v_r(M)$, is invariant under diffeomorphisms of $F \times I$ by the property of virtual links. Therefore whatever symplectic basis for the symplectic basis condition \mathcal{F} we take, we obtain the same value of our invariants v_r . This is an important property for our invariants v_r .

Remark: To actually apply our technique to a link L in $F \times I$ we need to associate to the link L embedded in $F \times I$ a framed virtual link diagram. The virtual Kirby class of this framed virtual diagram will then be an invariant of the the three-manifold $M(L)$, and it is assumed that L has been chosen so that the four manifold $W(L)$ is simply connected. As we have remarked, this condition of simple connectivity can be achieved by adding loops corresponding to the move \mathcal{O}_3 as illustrated in Figure 5.1. If the link L has originally been specified in $L \times I$ so that it satisfies the conditions of the Main Theorem, then one can obtain a virtual diagram for it, by taking a ribbon neighborhood of a blackboard framed projection to F and associating this with a virtual diagram in the standard way.

One can also start with a virtual diagram K and associate an embedding L in $F \times I$ by the reverse process. However, the resulting L may not satisfy the simple connectivity condition for the associated four-manifold. One way to insure this condition is to first associate a surface to K by adding a handle to the plane at each virtual crossing. Then augment K at each such handle to make sure that the simple connectivity condition is satisfied. In Figure 9.1 we show how this augmentation of loops corresponds to an augmentation of a virtual diagram at a virtual crossing. Here we interpret the virtual crossing as corresponding to a handle in the surface F . We illustrate the augmentation at that handle and show how it corresponds to adding virtual curves to the given virtual diagram K to form a virtual diagram K' . If we start with a virtual diagram K and apply this augmentation at each virtual crossing to form a virtual diagram K' , then resulting

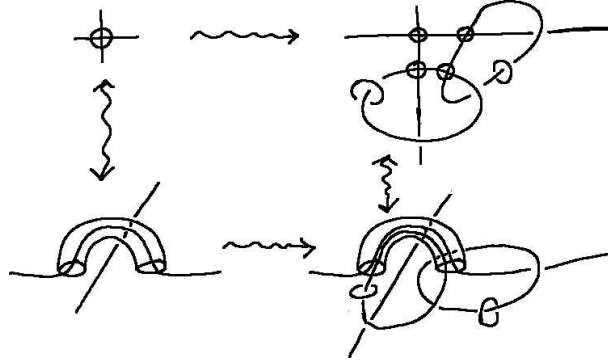


FIGURE 9.1. Virtual Augmentation

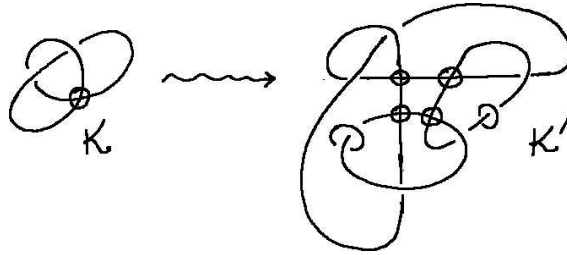


FIGURE 9.2. Virtual Augmentation Example

diagram K' will represent a three manifold $M(K')$ that satisfies the simple connectivity condition. Thus the virtual Kirby class of this diagram K' will be an invariant of the manifold $M(K')$. In this way we can create many examples for studying the results of this paper. In Figure 9.2 we illustrate a specific example K' whose invariants can be calculated. The reader interested in seeing the details of the calculation can consult [12, 4], apply the above description of the invariants and work out the expansion of the invariants for the link K' in Figure 9.2 .

10. Our topological quantum invariants v_r of classical knots in the 3-sphere

We define topological quantum invariants v_r of knots in the 3-sphere.

We make a knot K in S^3 into a 2-component link $L = (K, J)$ in S^3 as follows: J is the trivial knot. There is an embedded 2-disc in S^3 that J bounds and that K intersects geometrically once. Thus the linking number of K and J is one when we give an orientation to L . Then we say that $L = (K, J)$ is the *ring-hooked knot* of K . Note that the ring-hooked knot of K is determined by K uniquely. When K has a well-known

name, e.g., the trefoil knot, we abbreviate ‘the ring-hooked knot of the trefoil knot’ with ‘the ring-hooked trefoil knot’. The ring-hooked trivial knot is the Hopf link.

The complement of a ring-hooked knot (K, J) is a compact oriented 3-manifold whose boundary is the disjoint union of two tori. We can define our topological quantum invariants v_r for the complement if we induce the boundary condition \mathcal{B} . We put a symplectic basis for $\partial(S^3 - N(K \amalg J))$ in the next two paragraphs. Call this basis the *standard basis*.

We put a basis (u_1, v_1) for $K \times \partial D_2$ as follows: u_1 is defined by the meridian of K . v_1 is defined by a circle C embedded in $K \times \partial D_2$ such that C is homotopic to K in $K \times D^2$ and such that the linking number of K and C in the 3-sphere is zero.

We put a basis (u_2, v_2) for $J \times \partial D_2$ as follows: u_2 is defined by a circle E embedded in $J \times \partial D_2$ such that E is homotopic to J in $J \times D^2$ and such that the linking number of J and E in the 3-sphere is zero. v_2 is defined by the meridian of J .

Remark: We have $[u_1] = [u_2]$ and $[v_1] = [v_2]$ in $H_1(S^3 - N(K \amalg J); \mathbb{Z})$, where $u_1, u_2, v_1,$ and v_2 represent circles.

We define a topological quantum invariants v_r of each knot K to be our topological quantum invariants v_r of the complement of the ring-hooked knot of K with the above symplectic basis.

By our construction, v_r is a topological invariant of knots in the 3-sphere.

Part 2. Calculation

11. The simple connectivity condition is necessary to define our quantum invariants v_r

Figure 11.1 shows framed links A_1 and A_2 in the thickened torus. A_2 is obtained from A_1 by one \mathcal{O}_3 move. Therefore A_1 and A_2 represent the same 3-manifold with boundary, with the same boundary condition \mathcal{B} (Definition 2.1). We have the following.

Proposition 11.1. *In general, each of the Dye-Kauffman quantum invariants ς_r of A_1 is not equal to that of A_2 although A_1 and A_2 represent the same 3-manifold with boundary with the same boundary condition \mathcal{B} .*

Proof of Proposition 11.1. Calculation. See Table 15.1. □

Therefore we must concentrate on only framed links which satisfy the simple connectivity condition. We have the following observations.

Remark 11.2. *Let F be a connected closed oriented surface. Let M be a 3-manifold with boundary $F \amalg F$ with the boundary condition \mathcal{B} . Let L^{fr} and A^{fr} be framed links*

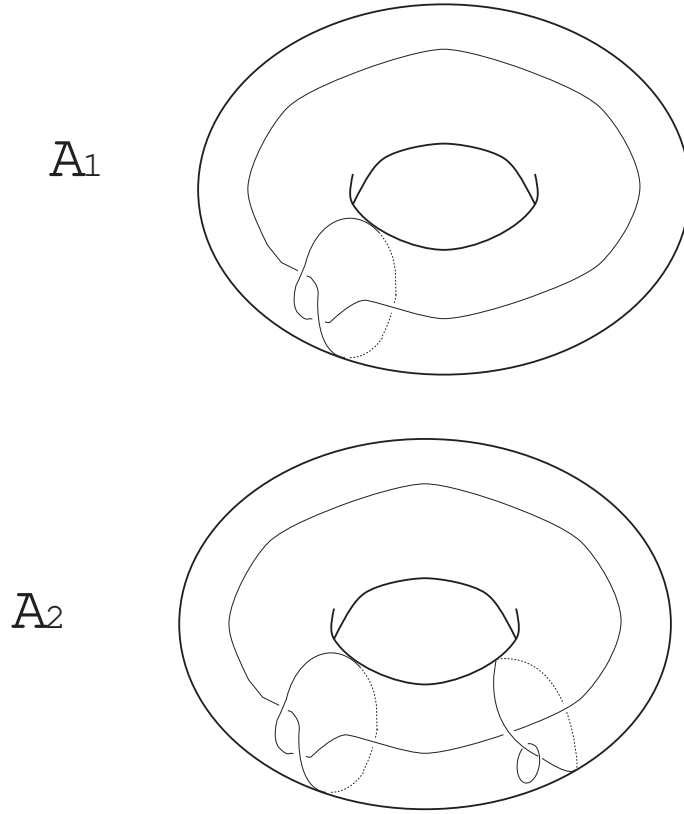


FIGURE 11.1. Framed links in thickened tori. All framings are zero.

in $F \times [-1, 1]$ with the symplectic basis condition \mathcal{F} which represent M . Assume that L^{fr} satisfies the simple connectivity condition but that A^{fr} does not satisfy it. Then, in general, each of the Dye-Kauffman quantum invariants ς_r of L^{fr} is not equal to that of A^{fr} .

Remark: Our quantum invariants v_r are not defined for A^{fr} because A^{fr} does not satisfy the simple connectivity condition. The Dye-Kauffman invariants ς_r are defined for A^{fr} and for all links in thickened surfaces because it is defined for all framed virtual links.

Remark 11.3. In general, the \mathcal{O}_3 move on framed virtual links changes the Dye-Kauffman quantum invariants ς_r for framed virtual links.

Remark 11.4. In Definition 9.1, the simple connectivity condition is necessary to define the our quantum invariants v_r .

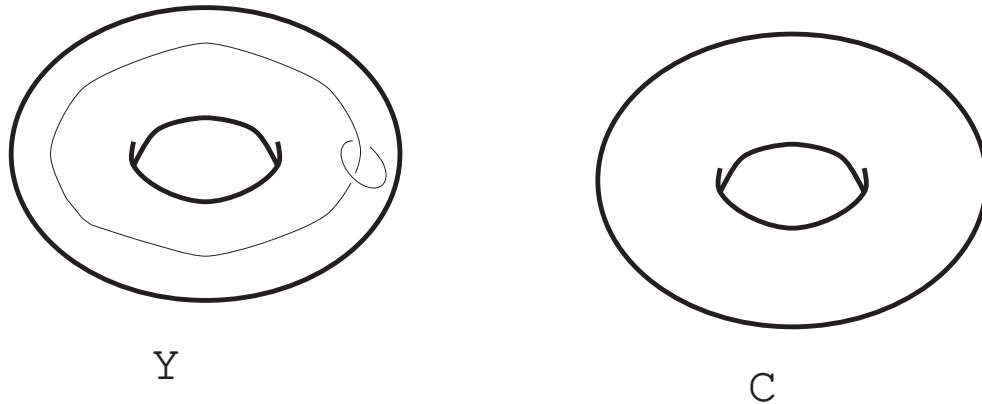


FIGURE 11.2. Framed links in thickened tori. All framings are zero.

Let L and L' be framed links in a thickened surface. Assume that L is obtained from L' by one \mathcal{O}_3 move.

If L and L' satisfy the simple connectivity condition, L is obtained from L' by a sequence of only the \mathcal{O}_1 and \mathcal{O}_2 moves. Recall Theorem 5.4. Therefore each of the Dye-Kauffman quantum invariants ς_r of L and that of L' are equivalent,

Remark 11.3 claims as follows: Assume the condition $(*)$ that one of L and L' does not satisfy the simple connectivity condition. In general, each of the Dye-Kauffman quantum invariants ς_r of L is not equivalent to that of L' .

However, under this condition $(*)$, it can happen that the \mathcal{O}_3 move does not change the Dye-Kauffman quantum invariants ς_r . See Figure 11.2. C is the empty framed link. Y is a 4-component framed link such that all framings are zero in the thickened torus. Y and C represent the same 3-manifold. Y and C represent different 4-manifolds such that their fundamental groups are different. Therefore Y is not obtained from C by a sequence of the \mathcal{O}_1 and the \mathcal{O}_2 moves. However, each of the Dye-Kauffman quantum invariants ς_r of C and that of Y are the same.

Reason: The virtual framed link representation of Y is the classical Hopf link such that both framings are zero. Therefore it is changed into the empty framed link by the \mathcal{O}_1 and the \mathcal{O}_2 moves.

See also the question in the last part of §15.

12. Framed links in complements of knots

As written in §1, in this paper, the *complement* of a link means as follows: Take a tubular neighborhood $N(L)$ of L . $N(L)$ is the open D^2 -bundle over L . The complement is defined to be $S^3 - N(L)$.

See Figure 12.1. The left upper figure is the complement of the trivial knot K , which includes a knot J . J is null-homologous in $S^3 - K$. Examine the top two diagrams in Figure 12.1. We attach a 4-dimensional 2-handle to the complement of K along J as follows. Since J is null-homologous in the complement of K , the framing of J makes sense. Let the framing be $+1$.

The result of this surgery is drawn in the right figure. It is the complement of the right-handed trefoil knot K' .

Remark: The complement of K is the solid torus. In general, we cannot define the linking number of 2-component links or the framing on knots in the solid torus. Recall §3.

However, the complement of K is embedded in the 3-sphere as drawn in Figure 12.1. The framing of J in the complement of K is specified by using the 3-sphere. Recall Remark 3.4. In Figure 12.1, these two ways of the definitions of framing coincide. *Reason:* Since J is null-homologous in the complement of K , there is a compact oriented surface F in the complement of K whose boundary is J . J is null-homologous in the 3-sphere and F is embedded in the 3-sphere. In both cases, the framing can be defined by using F .

As for the rest of the diagrams in Figure 12.1, the lower three figures are isotopic to the left upper figure. Thus one could have begun with the lowest diagram and pointed out that a surgery on the framed knot with framing $+1$ would produce the complement of the right-handed trefoil knot in the three sphere. We will use this kind of surgery in discussing links in thickened surfaces in the following sections.

13. Framed links in complements of 2-component links

We calculate examples of our topological quantum invariants v_r of knots in the 3-sphere defined in §10.

The first example is the right-handed trefoil knot. We make the ring-hooked right-handed trefoil knot (K'_1, K'_2) with the standard basis, (u_1, v_1) and (u_2, v_2) , (defined in §10) as drawn in the right upper figure of Figure 13.1. We have that $\partial(S^3 - N(K'_1 \amalg K'_2))$ is a disjoint union of two tori. In order to calculate our topological quantum invariants v_r , we construct a framed link in the thickened torus with the symplectic basis condition \mathcal{F} which represents $S^3 - N(K'_1 \amalg K'_2)$ with the standard basis as below.

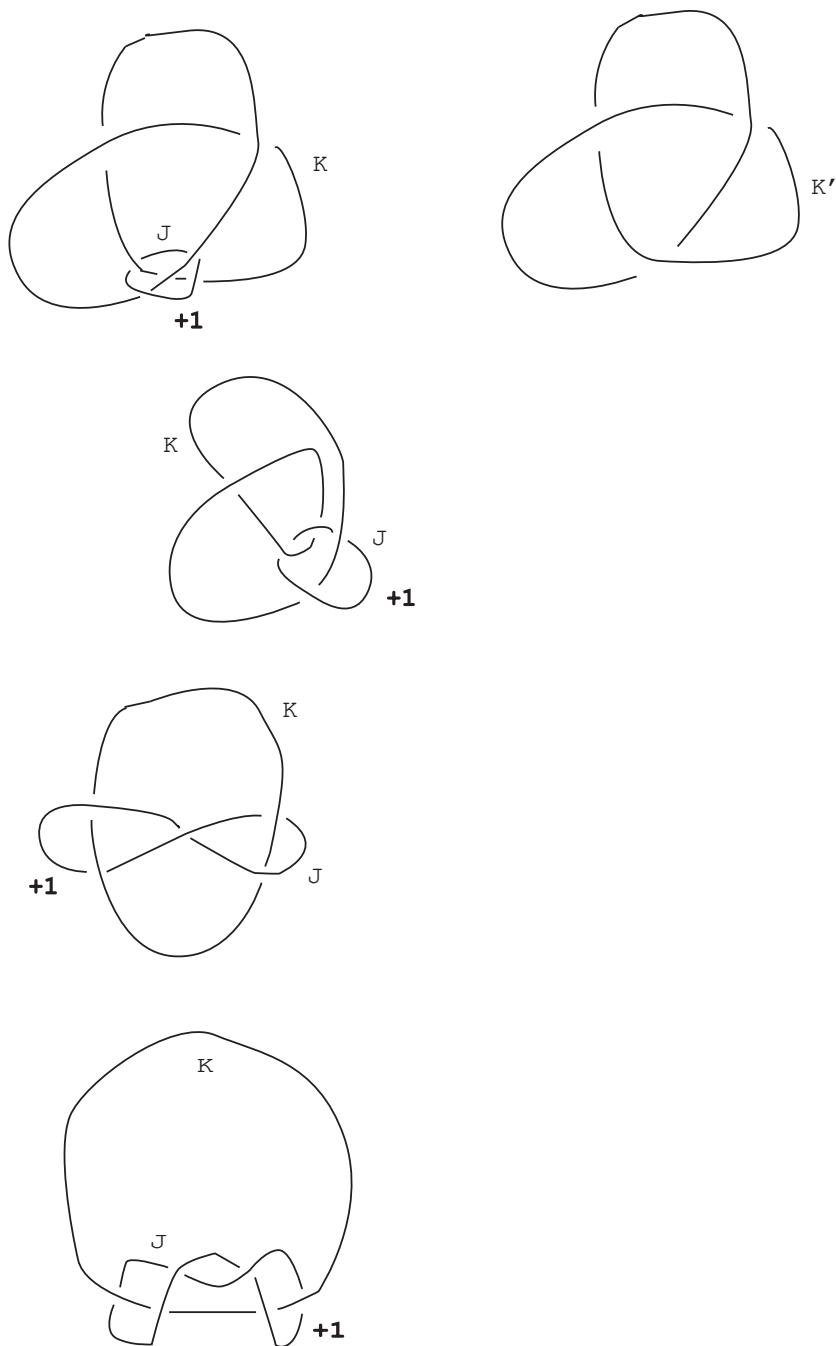


FIGURE 12.1. A ‘framed link’ in the complement of K and the result of the surgery

Take the ring-hooked trivial knot (K_1, K_2) . with the standard basis (p_1, q_1) in $\partial N(K_1)$ and (p_2, q_2) in $\partial N(K_2)$. Note that the complement of the ring-hooked trivial knot (K_1, K_2) is the thickened torus. The complement with the standard basis is the thickened torus with the symplectic basis condition \mathcal{F} . Recall Remark 9.3: Each of our topological quantum invariants v_r for any of the symplectic basis for the symplectic basis condition \mathcal{F} is the same.

The left upper figure in Figure 13.1 is the complement of the Hopf link (K_1, K_2) which includes the framed knot K with framing $+1$.

Note that framings make sense in the case of links in thickened surfaces as we review in §3. Since K is null-homologous, we can also define a framing on K by using the fact that the K is null-homologous. The framing is also $+1$.

We carry out $+1$ surgery along the framed knot on the complement of (K_1, K_2) . The result is drawn in the right figure. It is the complement of the ring-hooked right-handed trefoil knot (K'_1, K'_2) . Since K is null-homologous, the basis (p_1, q_1) (respectively, (p_2, q_2)) for K_1 (respectively, K_2) is changed into the basis (u_1, v_1) (respectively, (u_2, v_2)) for K'_1 (respectively, K'_2) after the surgery along J with framing $+1$. *Reason:* There is a compact oriented surface F_p (respectively, F_q) with boundary in $S^3 - N(K_1 \amalg K_2)$ whose boundary is p_1 and p_2 (respectively, q_1 and q_2). Note that F_p and F_q intersect. Since J is null-homologous in $S^3 - N(K_1 \amalg K_2)$, J never intersects F_p (respectively, F_q) algebraically.

The left middle figure is obtained from the left upper figure by an isotopy.

In the left lower figure, we draw a framed 5-component link in the complement of (K_1, K_2) : One component has framing $+1$ and the others have framings 0 . It is obtained from the framed link in the left middle figure by two times of the \mathcal{O}_3 move. Of course, both framed links represent the same 3-manifold.

Remark: The framed link in the left lower figure satisfies the simple connectivity condition. The one in the left middle figure does not.

Remark: Figure 13.1 draws a link (K_1, K_2) in the 3-sphere. The complement of (K_1, K_2) in the 3-sphere is the thickened torus. The framing of the knot by using the thickened torus, or the complement, is $+1$ (Recall §3).

The complement of (K_1, K_2) is embedded in the 3-sphere. We also specify the framing by using the 3-sphere. It is also $+1$.

Remark 13.1. Let Q be the complement of the Hopf link (K_1, K_2) as drawn in Figure 13.2. Here, note that the complement is the thickened torus and that Q is a submanifold of S^3 .

Take a framed knot J in Q whose framing is defined by using the thickened torus. We can also defined a framing on J by using S^3 because Q is a submanifold of S^3 .

In general, both methods do not give the same framing. See Figure 13.2. The boundary ∂Q is two tori. Take a collection X of circles in one of those two tori such that X and J

are homologous in Q . Since Q is a submanifold of the 3-sphere, the linking number ρ of (J, X) in the 3-sphere is determined uniquely by using the 3-sphere. Both methods give the same framing if and only if ρ is 0. In Figure 13.2, we have $\rho \neq 0$.

Framings in figures of this paper are defined by using the thickened surfaces.

The framed link in the left lower figure in Figure 13.1 is isotopic to that in Figure 13.3. These framed links, that in Figure 13.4, that in Figure 13.5, and that in Figure 13.6 represent the same 3-manifold with the same boundary condition \mathcal{B} and the same 4-manifold because they are changed into each other by handle slides. See Figure 13.6 and imagine a handle slide, which changes Figure 13.4 into Figure 13.5 (respectively, Figure 13.3 to Figure 13.4).

Figure 13.7 draws a framed link in the complement of the ring-hooked trivial knot, the Hopf link, (K_1, K_2) , which is the thickened torus with the standard basis in the boundary. Each component has the framing zero. This framed link represents the thickened torus with the same symplectic basis condition because this framed link is obtained by the \mathcal{O}_3 moves from the empty framed link. This framed link satisfies the simple connectivity condition.

We prove the following.

Theorem 13.2. *Our topological quantum knot invariants v_r are strong enough to distinguish some classical knots from one another.*

Corollary 13.3. *Our topological quantum invariants v_r are strong enough to distinguish some 3-manifolds with boundary where the boundary is a disjoint union of two identical surfaces, from one another.*

Proof of Theorem 13.2. Calculate our topological quantum knot invariants v_r of the right-handed trefoil knot by using a framed link drawn in the following figures: The lowest figure in Figures 13.1. Figures 13.3 - 13.6.

Calculate those of the trivial knot by using a framed link drawn in Figure 13.7. They are different by the result of Table 15.1. \square

Proof of Corollary 13.3. The pair which we calculate in Proof of Theorem 13.2 are also a pair to prove Corollary 13.3. \square

Therefore our topological quantum invariants v_r of knots and links are non-trivial invariants. Our topological quantum invariants v_r of 3-manifolds with boundary are non-trivial invariants.

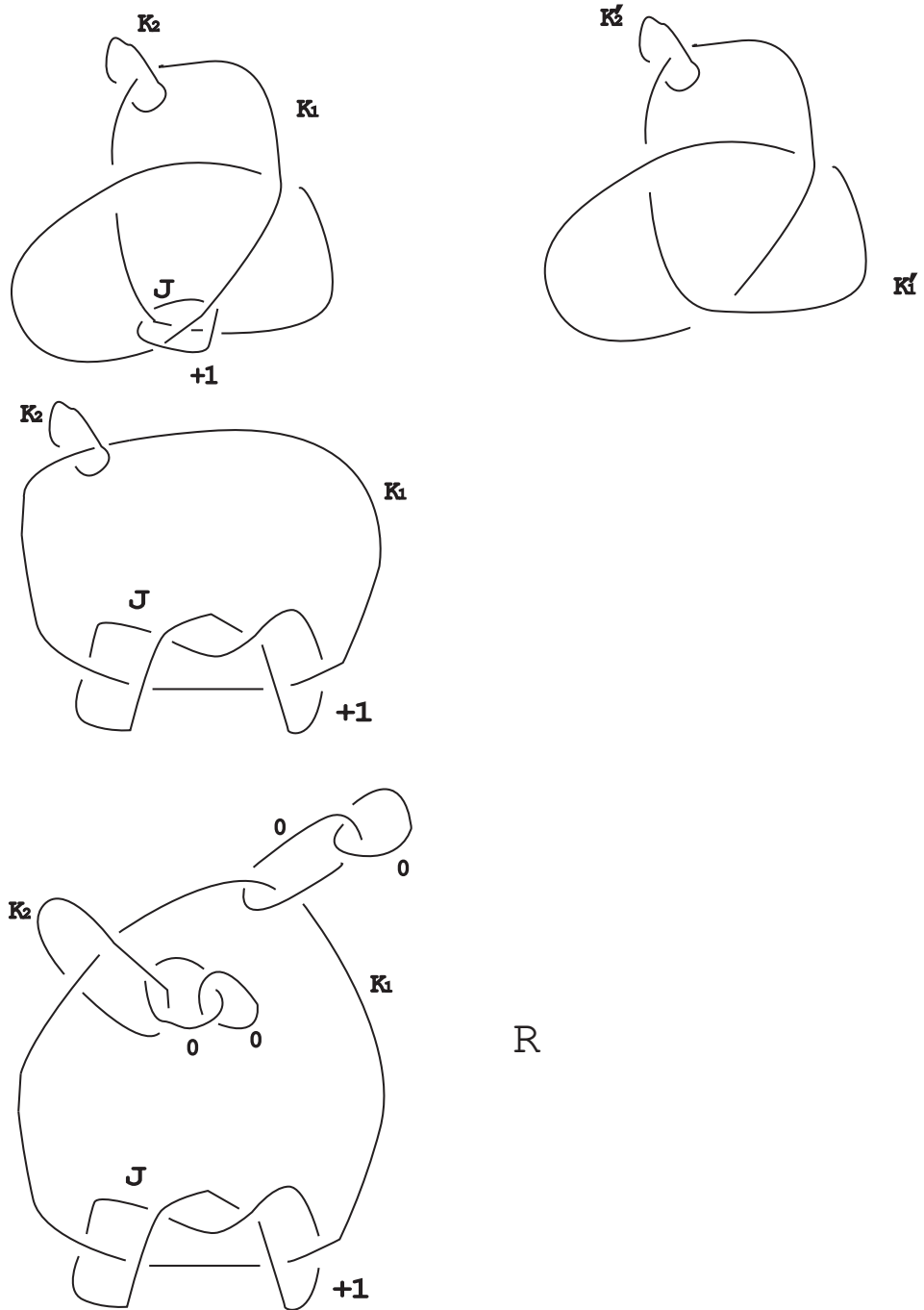


FIGURE 13.1. A ‘framed link’ in the complement of (K_1, K_2) and the result of the surgery

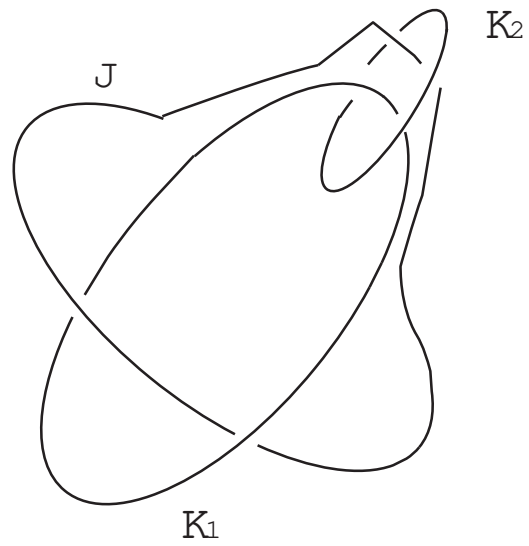


FIGURE 13.2. An example for Remark 13.1.

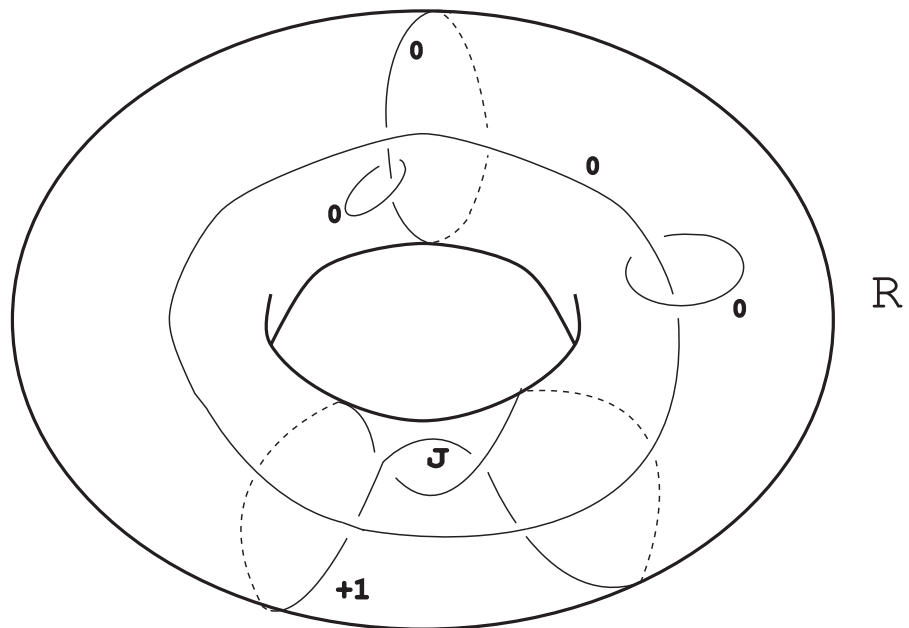


FIGURE 13.3. A framed link in the thickened torus

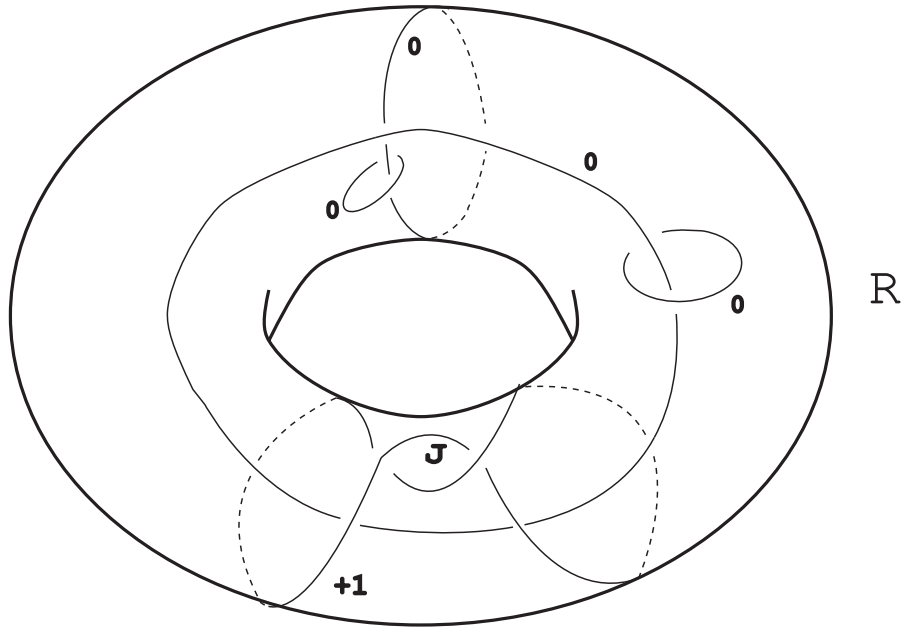


FIGURE 13.4. A framed link in the thickened torus

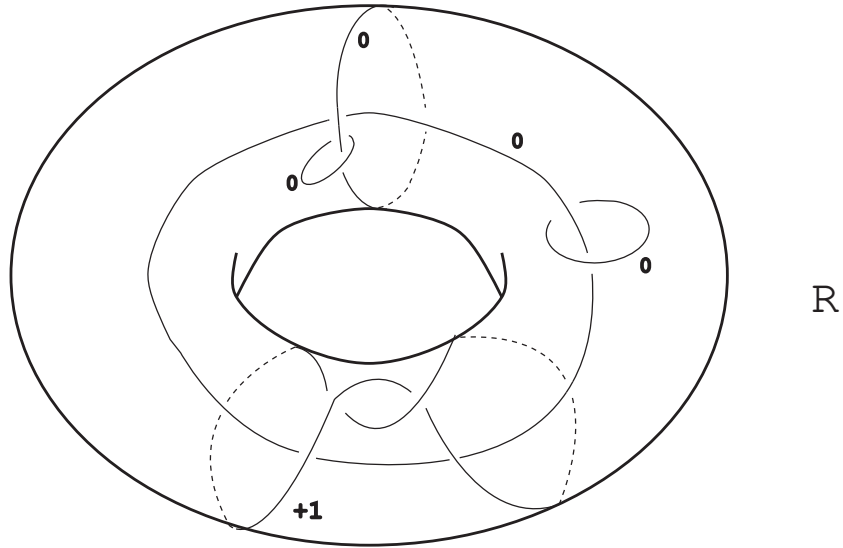


FIGURE 13.5. A framed link in the thickened torus

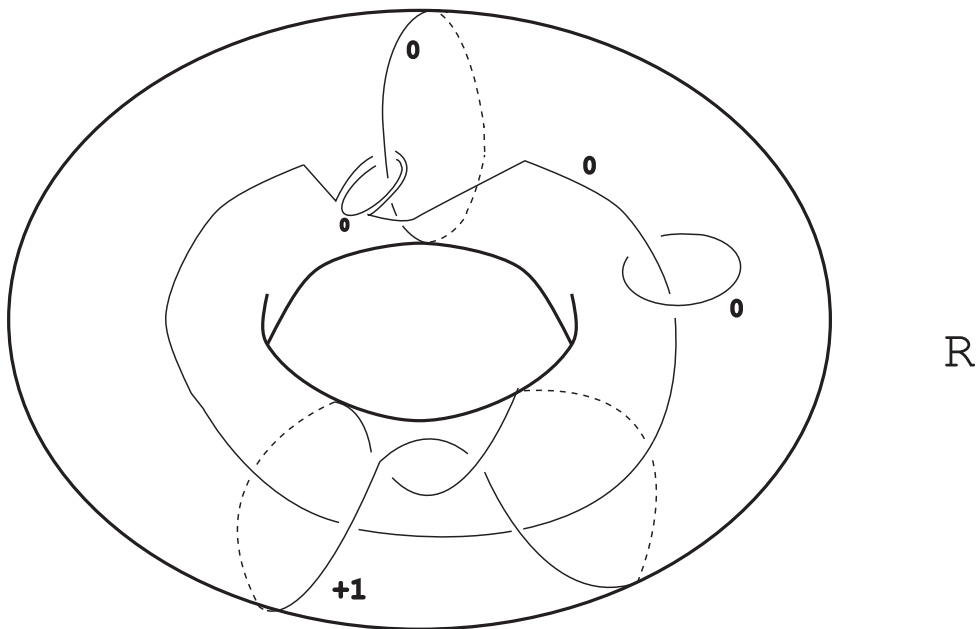


FIGURE 13.6. A framed link in the thickened torus

We explain how to calculate our invariant v_r of any other knot K than the trivial knot and the right-handed trefoil knot. We construct a framed link in the thickened torus with the symplectic basis condition \mathcal{F} , which represents the complement of the ring-hooked knot K with the standard basis as below. Let L be any given 2-component link. L may be a ring-hooked knot. Take a diagram D in S^2 of the Hopf link so that D satisfies the conditions: We put the ‘small trivial’ knots with framing ± 1 which is null-homologous in S^3 – (the Hopf link) as in Figure 12.1 at some crossing points of D . Whatever one uses the 3-sphere, the thickened torus, the fact that each ‘small knot’ is null-homologous, this framing is the same (Recall Remark 13.1). If we carry out surgeries along these ‘small trivial’ knots, then we get a diagram of L .

Then the framed link made from all of the above ‘small trivial’ knots is in the thickened torus. Using the \mathcal{O}_3 moves as drawn in Figure 5.1, we obtain a framed link which represents the complement of the ring-hooked knot with the standard basis and which satisfies the simple connectivity condition. We make it into a framed virtual link representation in the plane.

Remark: If we regard the Hopf link as a submanifold as drawn in the S^3 in Figure 12.1, each ‘small trivial’ knot looks the trivial knot. Indeed, in general, the ‘small trivial’ knot is not the trivial knot in the thickened torus.

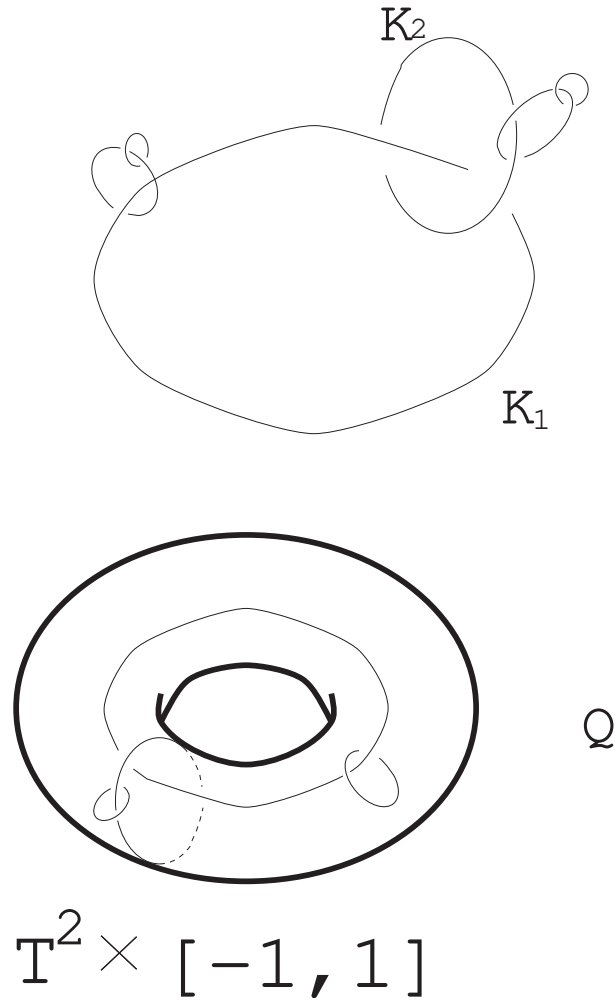


FIGURE 13.7. A framed link in the thickened torus

14. Our topological quantum invariants v_r is different from the Reshetikhin-Turaev topological quantum invariants τ_r

In Figure 14.1, we draw framed links, L_1 , L_2 , L_3 and L_4 . All components have the framing 0. They satisfy the simple connectivity condition. L_1 and L_2 (respectively, L_3 and L_4) are changed into each other by the \mathcal{O}_1 and \mathcal{O}_2 moves, without using a \mathcal{O}_3 move. L_1 and L_2 (respectively, L_3 and L_4) represent the same 3-manifold with boundary.

Remark: Q in Figure 13.7 and L_4 in Figure 14.1 are isotopic.

We prove the following proposition.

Proposition 14.1. *In general, each of our quantum invariants v_r of a 3-manifold with boundary, which is represented by a framed virtual link L_2 in Figure 14.1, is not equal to that by L_3 .*

Proof of Proposition 14.1. Calculation. See Table 15.1. □

Remark: Figure 14.1 draws the framed links, L_2 and L_3 , in the thickened torus. In Figure 14.1 the thickened torus is embedded in the 3-sphere. If we forget the thickened torus, we make framed links, L_2 and L_3 , in the thickened torus in Figure 14.1, into framed links, L'_2 and L'_3 , in the 3-sphere in Figure 14.2, respectively. Note that the framing of each component of L_2 (respectively, L_3) does not change when we forget the thickened torus (Recall Remark 13.1). Then both framed links L'_2 and L'_3 represent the 3-sphere. Therefore they have the same Reshetikhin-Turaev topological quantum invariant. Thus our topological quantum invariants v_r are different from the Reshetikhin-Turaev topological quantum invariants τ_r .

Furthermore, there are many ways to embed a thickened surface in \mathbb{R}^3 . Thus it does not determine a topological invariant to use an embedding of thickened surfaces in \mathbb{R}^3 and the Reshetikhin-Turaev topological quantum invariants as above.

On the other hand, our topological quantum invariants v_r are defined without using such an embedding.

In addition, recall that in the case of our invariants v_r of framed links in $F \times I$, the values, $v_r(M)$, are invariant under diffeomorphisms of $F \times I$. This is an important property for our invariants v_r that does not appear in the usual framework for WRT invariants τ_r . (Remark 9.3.)

See Figures 14.3 and 14.4 . A_0 is a framed knot with framing 0 in the thickened torus. If we regard the underlying knot as a virtual knot, it is the virtual right-handed trefoil knot.

A_1 is obtained from A_0 by an isotopy.

The framed links, A_1 and A_2 , represent the same 3-manifold. A_1 does not satisfy the simple connectivity condition although A_2 satisfies it.

The framed links, A_2 and J_1 , represent the same 3-manifold. Both A_2 and J_1 satisfies the simple connectivity condition.

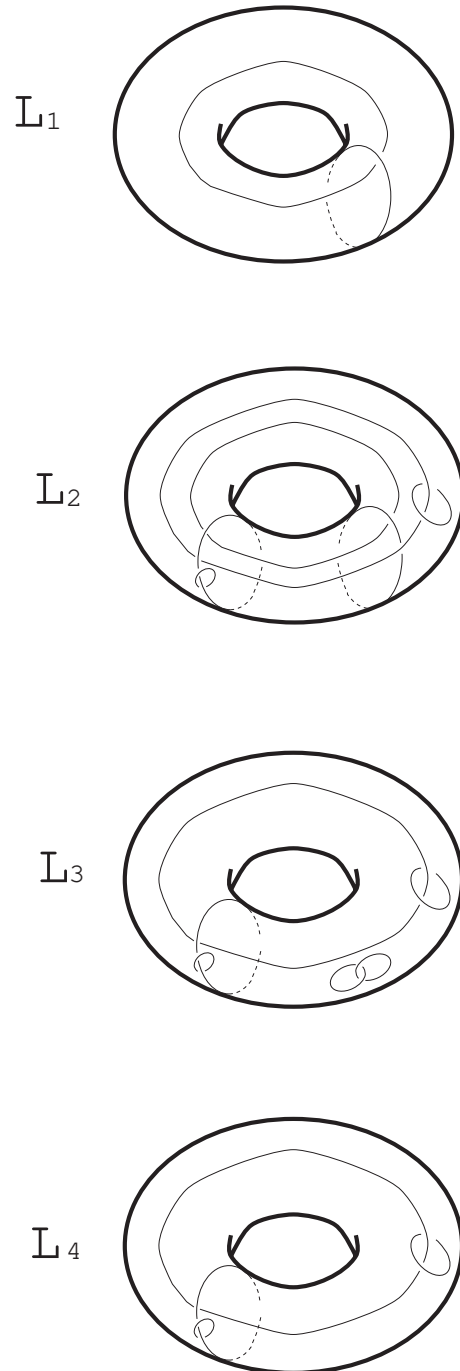


FIGURE 14.1. Framed links, L_1 , L_2 , L_3 , and L_4 , in the thickened torus. L_4 is isotopic to Q in Figure 13.7.

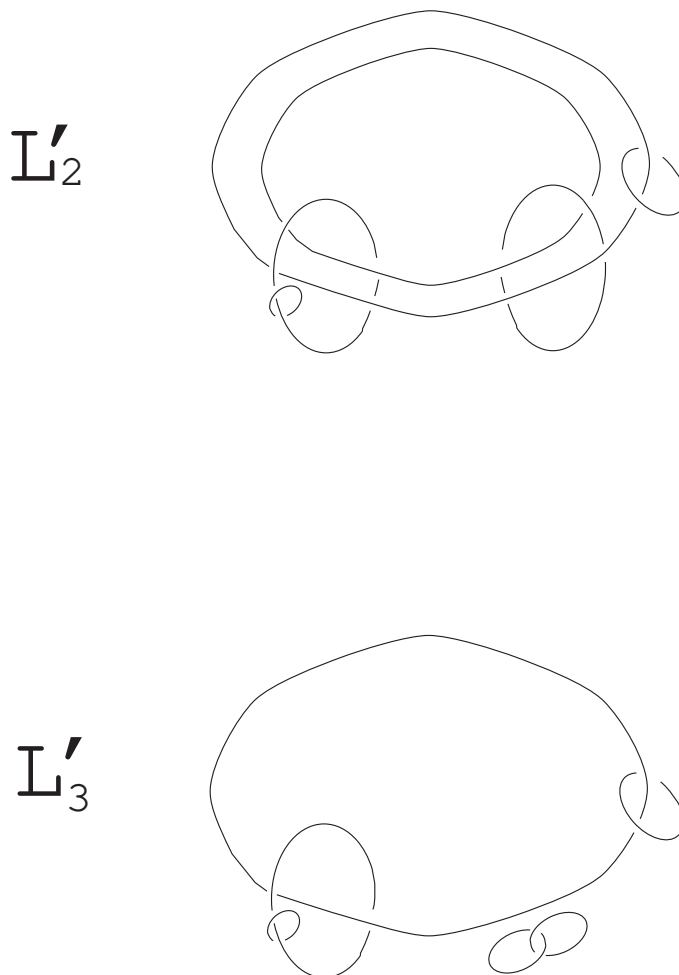


FIGURE 14.2. Framed links, L'_2 and L'_3 , in the 3-sphere

J_2 is a framed link in the thickened torus with the simple connectivity condition.

Remark: A_1 and A_2 in Figure 14.3 are the same as A_1 and A_2 in Figure 11.1, respectively.

We prove the following proposition.

Proposition 14.2. *Let J_1 and J_2 be as shown in Figure 14.4 and as discussed above. In general, each of our quantum invariants v_r of a 3-manifold with boundary, which is represented by J_1 , is not equivalent to that by J_2 .*

Proof of Proposition 14.2. Calculation. Table 15.1. □

Remark: Figure 14.4 draws the framed links, J_1 and J_2 . in the thickened torus. In Figure 14.4 the thickened torus is embedded in the 3-sphere. If we forget the thickened torus, we make framed links, J_1 and J_2 , in the thickened torus in Figure 14.4, into framed links, J'_1 and J'_2 , in the 3-sphere in Figure 14.5, respectively. Note that the framing of each component of J_1 (respectively, J_2) does not change when we forget the thickened torus (Recall Remark 13.1). Then both the framed links J'_1 and J'_2 represent the same 3-manifold. Therefore they have the same Reshetikhin-Turaev topological quantum invariant. Thus our topological quantum invariants v_r are different from the Reshetikhin-Turaev topological quantum invariants τ_r .

15. Calculation result

We calculate examples which we exhibited in this part, Part 2, explicitly. See Table 15.1.

The closure of the q-symmetrizer, denoted as Δ_n is the closure of a linear combination of elements in the Temperley-Lieb algebra and

$$(15.1) \quad \Delta_n = (-1)^n \frac{A^{2n} - A^{-2n}}{A^2 - A^{-2}}.$$

The recursive definition is utilized to evaluate the Kauffman-Ogasa invariant. The values of Δ_n for $n = 0$ and $n = -1$ are formally defined: $\Delta_{-1} = 0$ and $\Delta_0 = 1$. The symbol Δ_1 represents a single closed loop and $\Delta_1 = 1$. Then for $n > 0$,

$$(15.2) \quad \Delta_{n+1} = d\Delta_n - \Delta_{n-1}.$$

Each crossing in the knot diagram is transformed into a pair of trivalent vertices with labeled edges; shown in figure 15.1.

The labeled trivalent vertex represents a tangle as shown using the q-symmetrizer in figure 15.2. The edge labels must satisfy the equations

$$(15.3) \quad i = (a + b - c)/2, \quad j = (a + c - b)/2, \quad k = (b + c - a)/2.$$

The labeled link diagram is converted into a sum of weighted trivalent graphs where each labeled edge represents a q-symmetrizer. The graph can be successively simplified using the theta net and tetrahedral formulas given early in the paper. This is evaluated to a complex number by fixing an integer $r > 2$ and letting $A = e^{\frac{\pi i}{2r}}$. In this case, $\Delta_{r-1} = 0$. This, combined with the restriction on trivalent vertices, leads to admissibility restrictions on the labels of the diagrams. Non-admissible labels evaluate to zero.

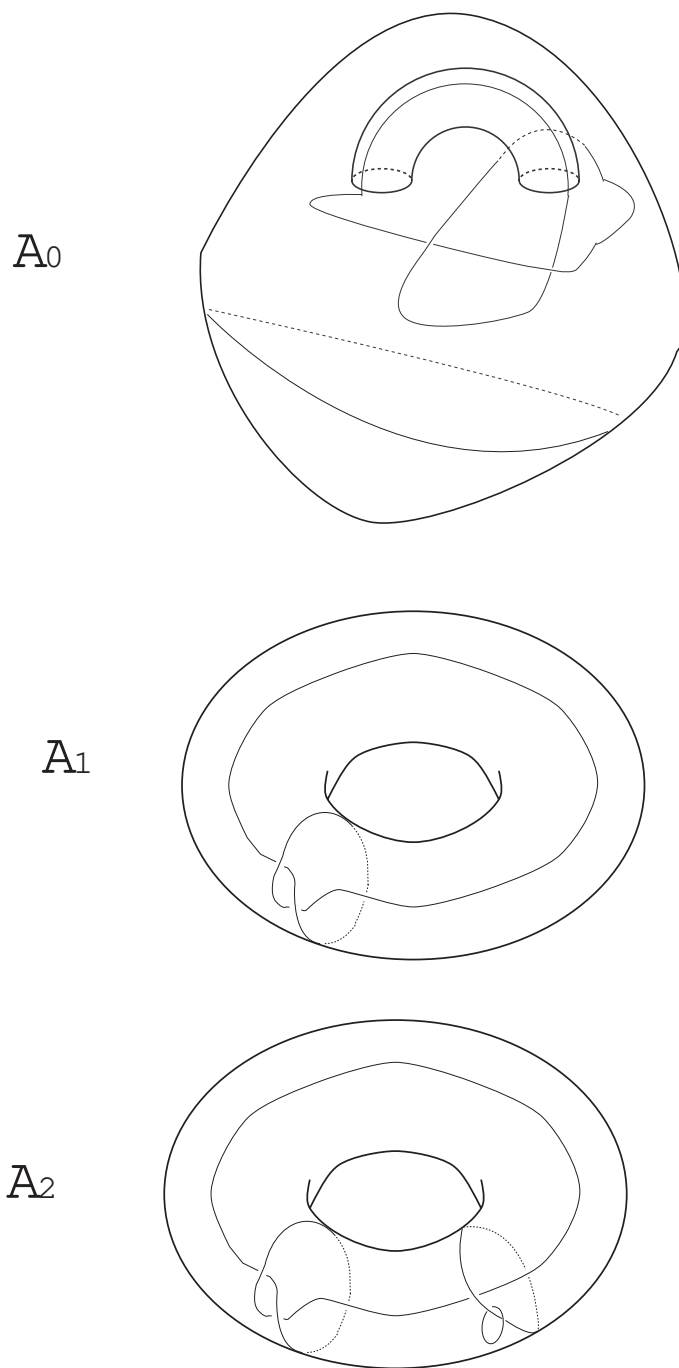


FIGURE 14.3. Framed links in the thickened torus

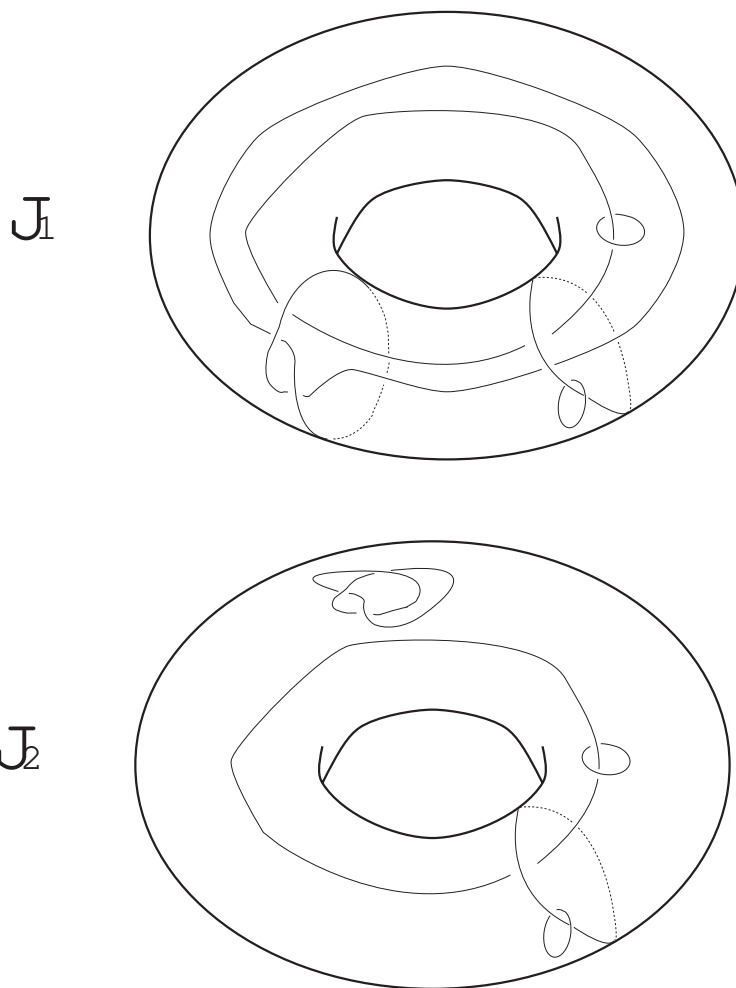


FIGURE 14.4. Framed links in the thickened torus

We summarize the admissibility requirement for any vertex in a diagram. For a fixed integer $r > 2$, any labeled edge must satisfy $0 \leq n \leq r - 2$. Combined with the vertex admissibility condition in equation 15.3, we obtain that $a + b + c \leq 2r - 4$ and $i, j, k \geq 0$.

For a virtual link diagram K obtained from a link in $F \times I$ and subject to the simple boundary condition, let c denote the number of components is c and let B denote the linking matrix. We let b_- (respectively b_+) denote the number of negative (respectively positive) eigenvalues of B . Then

$$(15.4) \quad Z(K) = \langle \omega * K \rangle \mu^{c+1} \alpha^{-(b_+ - b_-)}$$

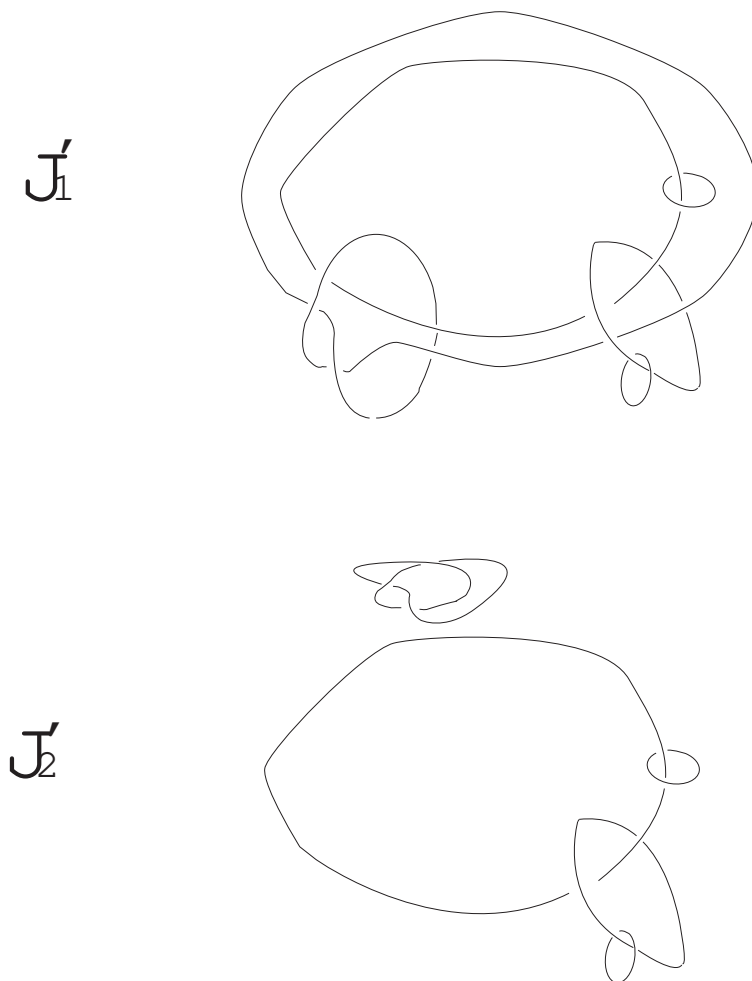


FIGURE 14.5. Framed links, J'_1 and J'_2 , in the 3-sphere

$$\begin{array}{c} \mathbf{a} \\ \diagdown \\ \diagup \\ \mathbf{b} \end{array} = \sum_{Adm(a,b,i)} \frac{\Delta_i}{\theta(a,b,i)} \lambda_i^{(ab)} \begin{array}{c} \mathbf{a} \quad \mathbf{b} \\ \diagdown \quad \diagup \\ \mathbf{i} \\ \diagup \quad \diagdown \\ \mathbf{a} \quad \mathbf{b} \end{array}$$

FIGURE 15.1. Converting link diagrams into graphs

where

$$\mu = \sqrt{\frac{2}{r}} \sin\left(\frac{\pi}{r}\right), \quad \alpha = (-i)^{r-2} e^{i\pi\left(\frac{3(r-2)}{4r}\right)}.$$



FIGURE 15.2. Expanding the trivalent vertex

For a single component diagram K , $\langle \omega * K \rangle = \sum_{i=0}^{r-2} \Delta_i K^i$ where K is labeled with i . Using this normalization, the $Z(U) = 1$ where U is the zero framed unknot.

Working with virtual link diagrams, we obtain elements of the virtual Temperley-Lieb algebra instead of the Temperley-Lieb algebra. As a result, our simplified diagrams contain virtual crossings and we are sometimes unable to completely reduce the diagrams to single loops. In the case that a reduced diagram has virtual crossings, we use symmetry and recursive evaluations of the q -symmetrizer to obtain a complex value.

Consider the virtual Hopf link H . Let a and b denote the labels placed on the components of the link. The linking matrix is

$$B = \begin{bmatrix} 0 & -1 \\ 0 & 0 \end{bmatrix}.$$

Then

$$(15.5) \quad Z(H) = \langle \omega * H \rangle \mu^3 \alpha^0.$$

We expand $\langle \omega * H \rangle$:

$$(15.6) \quad \langle \omega * H \rangle = \sum_{a,b=0}^{r-2} \Delta_a \Delta_b \text{ (diagram of two overlapping circles with a crossing) }.$$

We then exchange the crossing for an edge, constructing a trivalent graph

$$(15.7) \quad \sum_{Adm(a,b,i)} \Delta_a \Delta_b \frac{\Delta_i}{\theta(a,b,i)} \lambda_i^{ab} \text{ (diagram of two overlapping circles with an edge between them) }.$$

This diagram cannot be simplified further using the existing reduction formulas. The graph represents a collection of closed curves with virtual crossings. The graph in 15.7 is symmetric. Under the detour move, any pair of edges in the graph can contain the virtual crossing. We refer to this diagram as a *twisted theta*, $\tilde{\theta}(a,b,i)$.

Finally, we obtain the formula

$$(15.8) \quad \langle \omega * H \rangle = \sum_{Adm(a,b,i)} \Delta_a \Delta_b \Delta_i \frac{\tilde{\theta}(a,b,i)}{\theta(a,b,i)} \lambda_i^{ab}.$$

Note that $\tilde{\theta}(a, a, 0)$ evaluates to Δ_a for all values of a . Other values must be evaluated by hand.

We consider another example that cannot be reduced using the existing reduction formulas.

We evaluate the diagram A_2 from figure 14.3. This three component link has a linking matrix of the form:

$$(15.9) \quad \begin{bmatrix} 2 & 0 & 0 \\ 1 & 0 & 1 \\ 0 & 1 & 0 \end{bmatrix}.$$

Note that there are 2 positive eigenvalues and 1 negative eigenvalue. Therefore,

$$(15.10) \quad Z(A_2) = \mu^3 \alpha^{-1} \langle \omega * A_2 \rangle.$$

We reduce and evaluate $\langle \omega * A_2 \rangle$.

$$(15.11) \quad \langle \omega * A_2 \rangle = \sum_{a,b,c=0}^{r-2} \Delta_a \Delta_b \Delta_c \left\langle \begin{array}{c} \mathbf{a} \\ \mathbf{b} \\ \mathbf{c} \end{array} \right\rangle.$$

Next,

$$(15.12) \quad \langle \omega * A_2 \rangle = \sum_{\substack{Adm(a, a, j) \\ Adm(a, a, m) \\ Adm(b, c, i)}} \Delta_a \Delta_c \Delta_i (\lambda_i^{bc})^2 (\lambda_j^{aa})^2 (\lambda_n^{aa})^2 \frac{\Delta_m^2}{\theta(a, a, m)^3} \frac{\Delta_j}{\theta(a, a, j)}$$

$$Tet \begin{bmatrix} a & a & m \\ a & a & j \end{bmatrix} \left\langle \begin{array}{c} \mathbf{a} \\ \mathbf{b} \\ \mathbf{m} \end{array} \right\rangle.$$

The final reduction to a spatial graph results in the formula:

$$\langle \omega * A_2 \rangle = \sum_{\substack{Adm(a, a, j) \\ Adm(a, a, m) \\ Adm(b, c, i) \\ Adm(a, b, p)}} \Delta_a \Delta_c \Delta_i (\lambda_i^{bc})^2 (\lambda_j^{aa})^2 (\lambda_n^{aa})^2 \frac{\Delta_m^2}{\theta(a, a, m)^3} \frac{\Delta_j}{\theta(a, a, j)} \frac{\Delta_p}{\theta(a, b, p)}$$

$$Tet \begin{bmatrix} a & a & m \\ a & a & j \end{bmatrix} \left\langle \begin{array}{c} \mathbf{a} \\ \mathbf{b} \\ \mathbf{m} \\ \mathbf{p} \end{array} \right\rangle.$$

Note that the reduced graph has 4 vertices and forms a tetrahedral net structure with virtual crossings. This graph must be evaluated by hand to obtain an element of the algebra $\mathbb{Z}[A, A^{-1}]$. Fortunately, the figure has some symmetries, simplifying the evaluation.

Our computational results are in Table 15.1.

Future questions for research include finding a closed formula for $\tilde{\theta}(a, b, i)$ and the virtual tetrahedrons.

We calculate our topological quantum invariants v_r of the following 3-manifolds with the boundary condition \mathcal{B} . They are represented by framed links in the thickened torus with the symplectic basis condition \mathcal{F} .

A_1, A_2 in Figure 11.1.

Y, C in Figure 11.2.

R in Figures 13.1 and 13.3 - 13.6.

Q in Figure 13.7.

L_1, L_2, L_3, L_4 in Figure 14.1.

$$v_r(L_1) = v_r(L_2).$$

$$v_r(L_3) = v_r(L_4).$$

$$L_4 \text{ and } Q \text{ are isotopic. Hence } v_r(L_4) = v_r(Q).$$

A_0, A_1, A_2 in Figure 14.3.

$$A_0 \text{ and } A_1 \text{ are isotopic. Hence } v_r(A_0) = v_r(A_1).$$

A_1 and A_2 in Figure 14.3 are the same as A_1 and A_2 in Figure 11.1, respectively.

J_1, J_2 in Figure 14.4.

$$v_r(A_2) = v_r(J_1).$$

X, A , and B are introduced right below.

We ask a question. See Figure 15.3. C represents the empty framed link. X, A, B , and C represent the same 3-manifold.

X is obtained from A by a sequence of only the \mathcal{O}_1 and the \mathcal{O}_2 moves.

B is obtained from C by a sequence of only the \mathcal{O}_1 and the \mathcal{O}_2 moves.

A is not obtained from B without using the \mathcal{O}_3 move because their fundamental groups

Framed link	$r = 3$	$r = 4$	$r = 5$
L_1, L_2	$1.06066 - 0.353553 i$	$0.0967185 + 1.20711 i$	$0.553238 + 1.04288 i$
$L_3, L_4, Q, X, Y, A, B, C$	0.707107	0.5	0.37148
A_1	$0.707107 + 0.707107 i$	$-1.30656 + 0.92388 i$	$-1.58479 - 1.72679 i$
A_2, J_1	$-0.25 + 0.103553 i$	$0.0544203 - 0.253256 i$	
J_2	$0.707107 i$	$0.353553 - 0.353553 i$	$-0.158114 + 0.716377 i$
R	-0.707107	0	$0.352125 - 0.484658i$

TABLE 15.1. Computational Results.

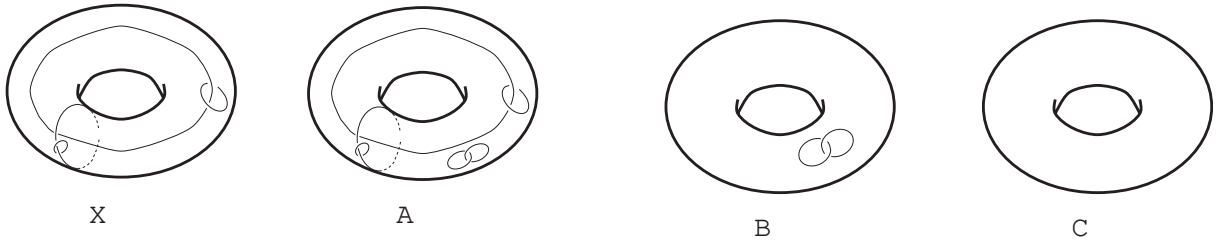


FIGURE 15.3. Framed links in thickened tori. All framings are zero. Note that A in Figure 15.3 is L_3 in Figure 14.1, and that X in Figure 15.3 is L_4 in Figure 14.1.

are different. Therefore A is not obtained from B by a sequence of the \mathcal{O}_1 and the \mathcal{O}_2 moves.

X and A satisfy the simple connectivity condition while B and C do not.

Each of the Dye-Kauffman quantum invariants ς_r of X and that of A are the same because X is obtained from A by the \mathcal{O}_1 and the \mathcal{O}_2 moves.

Each of the Dye-Kauffman quantum invariants ς_r of B and that of C are the same because B is obtained from C by the \mathcal{O}_1 and the \mathcal{O}_2 moves.

C in Figure 15.3 is the same as C in Figure 11.2.

$$v_r(X) = v_r(A).$$

$$v_r(B) = v_r(C).$$

A in Figure 15.3 is L_3 in Figure 14.1.

X in Figure 15.3 is L_4 in Figure 14.1.

In the case of $r = 3, 4, 5$, the Dye-Kauffman invariants ς_r of X , A , B , and C have the same apparent value. See Table 15.1.

Question. Are the Dye-Kauffman quantum invariants ς_r of X , A , B , and C the same for all r ?

Appendix

We discuss some open questions.

Reshetikhin and Turaev [33, Theorem 3.3.3, page 560] defined invariants for links in a closed oriented 3-manifold M . These invariants depend on the use of the colored Jones polynomials at roots of unity and the use of the Kirby calculus. If $M = S^3$, these invariants are invariants of links in S^3 .

Apply the definition in [33, Theorem 3.3.3, page 560] strictly to the case of S^3 . The readers can understand easily that the definition of these invariants is different from that of the Jones polynomial.

It is an open question whether these invariants retrieves the Jones polynomial.

The following two questions both are open.

Question A.1. Suppose that these invariants of a link \mathcal{L} in S^3 and those of \mathcal{L}' in S^3 are the same. (We may not be able to know the coincidence by a finite times of operation. We may just suppose this condition abstractly.) Then are the Jones polynomial of \mathcal{L} and that of \mathcal{L}' the same?

Question A.2. By a finite times of explicit calculation of (a partial information of) these invariants of a link \mathcal{L} in S^3 , can we determine the Jones polynomial of \mathcal{L} ?

We have not known whether the Reshetikhin-Turaev invariants of links in any 3-manifold is an extension of the Jones polynomial of links in S^3 .

We have another open question.

Question A.3. Calculate Witten's well-known path integral for links in other 3-manifolds than S^3 .

Remark: Witten calculated only the S^3 case. See [40].

Even in the 'physics' level, the Jones polynomial has not been extended to all 3-manifold cases. Witten only wrote a Lagrangian and an observable for a path integral, in

the case of links in all (closed oriented) 3-manifolds. Only writing a path integral never means that the path integral has been calculated. Before calculating it explicitly (in the ‘physics’ level), we cannot say that the path integral defines a value.

Recall a current situation of QCD and a history of QED. Before Tomonaga, Feynman and Schwinger discovered renormalization, we wrote a well-known Lagrangian and wrote path integral for QED. We write a well-known Lagrangian and write path integral for QCD, but we cannot say that we complete QCD.

It is also an open question whether Khovanov homology ([2, 17]) and Khovanov-Lipshitz-Sarkar homotopy type ([25, 26, 27, 37]) are extended to the case of links in any other 3-manifold than the 3-sphere. Both are now extended only to the case of thickened surfaces. See the case of Khovanov homology for Asaeda, Przytycki, and Sikora [1], Manturov [28] (arXiv 2006), Rushworth [36], Tubbenhauer [38], and Viro [39]. Manturov and Nikonov [30] refined the definition of [1]. Dye, Kastner, and Kauffman [3], Nikonov [31], and Kauffman and Ogasa [13] refined the definition of [28]. Kauffman and Ogasa [13] extended the second Steenrod square acting on Khovanov homology for links in S^3 to the case of thickened surfaces. Kauffman, Nikonov and Ogasa [15, 16] extended Khovanov-Lipshitz-Sarkar stable homotopy type to the case of thickened surfaces. Some of them are defined by using virtual links.

REFERENCES

- [1] M. M. Asaeda, J. H. Przytycki, and A. S. Sikora; Categorification of the Kauffman bracket skein module of I -bundles over surfaces, *Algebraic & Geometric Topology* 4 (2004) 11771210 ATG
- [2] D. Bar-Natan: On Khovanov’s categorification of the Jones polynomial, *Algebr. Geom. Topol.* 2(2002), 337370 (electronic). MR 1917056 (2003h:57014).
- [3] H A Dye, A Kaestner, and L H Kauffman: Khovanov Homology, Lee Homology and a Rasmussen Invariant for Virtual Knots, *Journal of Knot Theory and Its Ramifications* 26 (2017).
- [4] H. A. Dye, and L. H. Kauffman: Virtual Knot Diagrams and the Witten-Reshetikhin-Turaev Invariant, arXiv:math/0407407
- [5] R. A. Fenn, and C. P. Rourke: On Kirby’s calculus of links, *Topology* 18 (1979), 1-15.
- [6] D. P. Ilyutko and V. O. Manturov: Virtual Knots: The State of the Art, *World Scientific Publishing Co. Pte. Ltd.* 2012. English translation of [29].
- [7] V. F. R. Jones: Hecke Algebra representations of braid groups and link *Ann. of Math.* 126 (1987) 335-388.
- [8] L. H. Kauffman: Talks at MSRI Meeting in January 1997, AMS Meeting at University of Maryland, College Park in March 1997, Isaac Newton Institute Lecture in November 1997, Knots in Hellas Meeting in Delphi, Greece in July 1998, APCTP-NANKAI Symposium on Yang-Baxter Systems, Non-Linear Models and Applications at Seoul, Korea in October 1998
- [9] L. H. Kauffman: Knots and Physics *Series on Knots and Everything, Vol. 1, World Scientific* 1991, 1994, 2001.

- [10] L. H. Kauffman: Virtual Knot Theory, *Europ. J. Combinatorics* (1999) 20, 663691, *Article No. eujc.1999.0314*, Available online at <http://www.idealibrary.com/math/9811028> [math.GT].
- [11] L. H. Kauffman: Introduction to virtual knot theory *J. Knot Theory Ramifications* 21 (2012), no. 13, 1240007, 37 pp.
- [12] L. H. Kauffman and S. L. Lins: Temperley-Lieb Recoupling Theory and Invariants of 3-Manifolds *Annals of Mathematics Studies, Princeton University Press* (1994).
- [13] L. H. Kauffman and E. Ogasa: Steenrod square for virtual links toward Khovanov-Lipshitz-Sarkar stable homotopy type for virtual links, arXiv:2001.07789 [math.GT].
- [14] L. H. Kauffman and E. Ogasa: Quantum Invariants of Links and 3-Manifolds with Boundary defined via Virtual Links, arXiv 2108.13547 math.GT
- [15] L. H. Kauffman, I. M. Nikonov, and E. Ogasa: Khovanov-Lipshitz-Sarkar homotopy type for links in thickened higher genus surfaces arXiv: 2007.09241[math.GT].
- [16] L. H. Kauffman, I. M. Nikonov, and E. Ogasa: Khovanov-Lipshitz-Sarkar homotopy type for links in thickened surfaces and those in S^3 with new modulus, arXiv:2109.09245 [math.GT].
- [17] M. Khovanov. A categorification of the Jones polynomial. *Duke Mathematical Journal*, 101, 1999.
- [18] R. C. Kirby: A calculus for framed links in S^3 *Invent. Math.* 45 (1978), 35-56.
- [19] R. C. Kirby: The topology of 4-manifolds *Lecture Notes in Math (Springer Verlag)* vol. 1374, 1989
- [20] R. C. Kirby and P. Melvin: The 3-manifold invariants of Witten and Reshetikhin-Turaev for $sl(2, C)$ *Inventiones Mathematicae* 105 (1991) 473545.
- [21] G. Kuperberg: What is a virtual link? *Algebr. Geom. Topol.* 3 (2003) 587-591.
- [22] W. B. R. Lickorish: A representation of orientable combinatorial 3-manifolds *Ann. Math.* 76 (1962), 531-540.
- [23] W. B. R. Lickorish: Invariants for 3-manifolds from the combinatorics of the Jones polynomial *Pacific J. Math.* 149 (1991) 337-347.
- [24] W. B. R. Lickorish: Three-manifolds and the Temperley-Lieb algebra *Mathematische Annalen* 290 (1991) 657670.
- [25] R. Lipshitz and S. Sarkar: A Khovanov stable homotopy type, *J. Amer. Math. Soc.* 27 (2014), no. 4, 9831042. MR 3230817
- [26] R. Lipshitz and S. Sarkar: A Steenrod square on Khovanov homology, *J. Topol.* 7 (2014), no. 3, 817848. MR 3252965
- [27] R. Lipshitz and S. Sarkar: A refinement of Rasmussen's s-invariant, *Duke Math. J.* 163 (2014), no. 5, 923952. MR 3189434.
- [28] V O Manturov: Khovanov homology for virtual links with arbitrary coefficients, *Journal of Knot Theory and Its Ramifications* 16 (2007).
- [29] V. O. Manturov: Virtual Knots: The State of the Art, (*in Russian*) 2010.
- [30] V. O. Manturov and I. M. Nikonov: Homotopical Khovanov homology *Journal of Knot Theory and Its Ramifications* 24 (2015) 1541003.
- [31] I. M. Nikonov: Virtual index cocycles and invariants of virtual links, arXiv:2011.00248
- [32] E. Ogasa: An elementary introduction to Khovanov-Lipshitz-Sarkar stable homotopy type, <https://www.researchgate.net/publication/352136009> - An elementary introduction to Khovanov-Lipshitz-Sarkar stable homotopy type (The readers can find this article by typing in the title in a search engine.)
- [33] N. Reshetikhin and V. G. Turaev: Invariants of 3-manifolds via link polynomials and quantum groups, *Inventiones mathematicae* 103 (1991) 547597.

- [34] N. Reshetikhin and V. G. Turaev: Ribbon Graphs and their invariants derived from quantum groups, *Communications in Mathematical Physics*, 127(1990) 1-26.
- [35] J. Roberts: Kirby calculus in manifolds with boundary *Proceedings of 5th Gkova. Geometry-Topology Conference*.21(1997)111-117, arXiv:math/9812086.
- [36] W. Rushworth: Doubled Khovanov Homology, *Can. j. math.* 70 (2018) 1130-1172.
- [37] C. Seed: Computations of the Lipshitz-Sarkar Steenrod square on Khovanov homology, arXiv:1210.1882.
- [38] D. Tubbenhauer: Virtual Khovanov homology using cobordisms, *J. Knot Theory Ramifications* 23 (2014), no. 9, 1450046, 91 pp.
- [39] Viro; Khovanov homology of Signed diagrams 2006 (an unpublished note).
- [40] E. Witten: Quantum field theory and the Jones polynomial *Comm. Math. Phys.* 121 (1989) 351-399.

Heather A. Dye
 Division of Science and Math
 McKendree University
 701 College Rd.
 Lebanon, IL 62254
 USA
 heatheranddye@gmail.com

Louis H. Kauffman
 Department of Mathematics, Statistics and Computer Science
 University of Illinois at Chicago
 851 South Morgan Street
 Chicago, Illinois 60607-7045
 USA
 kauffman@uic.edu

Eiji Ogasa
 Meijigakuin University, Computer Science
 Yokohama, Kanagawa, 244-8539
 Japan
 pqr100pqr100@yahoo.co.jp
 ogasa@mail1.meijigakuin.ac.jp